Neutrino Oscillations

May 3, 2016

Contents

1 Introduction

This section discusses the phenomenon of neutrino flavour oscillations, the big discovery of the last 10 years, which prompted the first major change to the standard model in the last 20 years. We will discuss the evidence for neutrino oscillations, look at the formalism - both for 2-flavour and 3-flavour oscillations, and look at oscillation experiments.

This is a long document - where possible I will try to point out what you should know and what you don't necessarily need for an exam.

2 Neutrino Flavour Oscillation in Words

I will first introduce the concept of neutrino flavour oscillations without going into the rigorous theory (see below). We have seen that the thing we call a neutrino is a state that is produced in a weak interaction. It is, by definition, a flavour eigenstate, in the sense that a neutrino is always produced with, or absorbed to give, a charged lepton of electron, muon or tau flavour. The neutrino that is generated with the charged electron is the electron neutrino, and so on. However, as with the quarks and the CKM matrix, it is possible that the flavour eigenstates (states with definite flavour) are not identical to the mass eigenstates (states which have definite mass).

What does this mean? Suppose we label the mass states as ν_1, ν_2 and ν_3 and that they have different, but close, masses. Everytime we create an electron in a weak interaction we will create one of these mass eigenstates (ensuring the energy and momentum is conserved at the weak interaction vertex as we do so). Suppose that we create these with different probabilities (i.e. 10% of the time we create a ν_1 etc). If we could resolve the mass of each state, we could follow each mass state as it propagates. However, the neutrino masses are too small to experimentally resolve them. We know we created one of them, but not which one, so what we create, at the weak interaction vertex, is a coherent superposition of the ν_i mass states - this coherent superposition we call the *electron* neutrino :

$$|\nu_e >= U_{e1}|\nu_1 > +U_{e2}|\nu_2 > +U_{e3}|\nu_3 > \tag{1}$$

If this is the case, the following can happen : suppose one generates a neutrino at a source. This neutrino will have definite flavour, but will be produced as a linear combination of states of definite mass. The states of definite mass will propagate out of the source towards the detector. If the states have different masses, then the phase between the states will change with distance from the source (we will make this clear soon). At the detector, the mass states will have different relative phases to those the mass states had at the source, and when we go to detect them, it is possible that we will detect a flavour state which was not present in the beam to begin with. If one restricts oneself to two-flavour oscillations, we find that the probability of starting with one flavour, say ν_α, at the source but detecting another, say ν_β, at the detector is

$$P(\nu_\alpha \to \nu_\beta) = sin^2(2\theta) sin^2(1.27\Delta m^2 \frac{L(km)}{E(GeV)}) \tag{2}$$

This equation has a number of points of interest

- **The angle θ:** this is the so-called *mixing angle*. It defines how different the flavour states are from the mass states. If θ=0, the flavour states are identical to the mass states (that is, the ν_α will propagate from source to detector *as a* ν_α with definite momentum. Clearly in this case,

oscillations cannot happen. If $\theta = \frac{\pi}{4}$ then the oscillations are said to be *maximal* and at some point along the path between source and detector *all* of the ν_α we started with will oscillate to ν_β.

- **The mass squared difference, Δm^2 :** If there are 2 flavours there will be 2 mass states. This parameter is the difference in squared masses of each of these states : $\Delta m^2 = m_1^2 - m_2^2$. For neutrino oscillations to occur, at least one of the mass states must be non-zero. This simple statement has huge implications - for oscillations to happen, the neutrino **must have mass**. Furthur the masses of the mass states must be different, else $\Delta m^2 = 0$ and $P(\nu_\alpha \rightarrow \nu_\beta) = 0$. You can see why this is : the masses control the relative phase of the two mass wavefunctions. If they are the same, then the mass states will never get out of phase and you will measure the same linear combination of mass states at the detector as you generated at the source. Note also the limitation of neutrino oscillation experiments - they can give us detailed information on the difference between the mass values, but *cannot* tell us what the absolute mass of the states are. Neither can they tell us whether m_1 is larger in mass than m_2. If $\Delta m^2 \rightarrow -\Delta m^2$ the probability will still be the same.

- **L/E :** This is the parameter we, as experimentalists control. L is the distance between the source and the detector, and E is the energy of the neutrino. For a given Δm^2, the probability of oscillation will change as one moves away from the detector, or scans over different neutrino energy. Experimentally, if we suspect that Δm^2 has a particular value, then we should build our experiment to be maximally sensitive to the oscillation probability. That is, we want to build it such that

$$1.27\Delta m^2 \frac{L}{E} = \frac{\pi}{2} \tag{3}$$

or

$$\frac{L}{E} = \frac{\pi}{2.54\Delta m^2} \tag{4}$$

. We are free then to either change the beam energy, or the baseline (L), or both. Ideally we want to maximise L and minimise E. This all sounds very nice, but practicalities tend to intrude. Neutrino beams diverge like an electric field from a point source, so the surface area of a detector placed at a distance L has to grow by L^2, and so does the cost. At the same time, the neutrino cross-section decreases as the neutrino energy decreases and so the running time to collect a useful number of events increases linearly (and so does the cost).

On the flip-side, if $\frac{L}{E}$ is fixed for us by nature (as it is, for example, in solar neutrinos), then we can only probe a certain range of $(\Delta m^2, \theta)$ combinations, since other choices for the values of these parameters will yield too small a probability of oscillation for observation to be feasible (we may have to wait decades to get enough events).

There are two types of neutrino oscillation experiments one could think of doing. The first is to start with a pure beam of known flavour ν_α, and look to see how many have disappeared. This is a "disappearance" experiment and measures the survival probability : $P(\nu_\alpha \rightarrow \nu_\alpha) = 1 - sin^2(2\theta) sin^2(1.27\Delta m^2 \frac{L(km)}{E(GeV)})$. The second type of experiment is an "appearance" experiment, in which one starts with a pure beam of known flavour ν_α and looks to see how many neutrinos of a different flavour ν_β are detected.

OK, that's a bunch of handwaving, but for the purposes of the historical account below will do.

3 Evidence for Neutrino Flavour Oscillations

3.1 Solar Neutrinos and the Solar Neutrino Problem

We discussed solar neutrino generation in the previous handout. The solar neutrino flux derived from Bahcall's Standard Solar Model is shown in Figure 1 for reference.

The Standard Solar Model predicts that most of the flux comes from the pp neutrinos with energies below 0.4 MeV. Only the Gallium experiements are sensitive to this component. The Chlorine experiments can just observe part of the ^7Be line, and can see the other components. The big water experiments (Super-Kamiokande, SNO) can only view the ^8B neutrinos as they have too high a threshold to see below about 5 MeV.

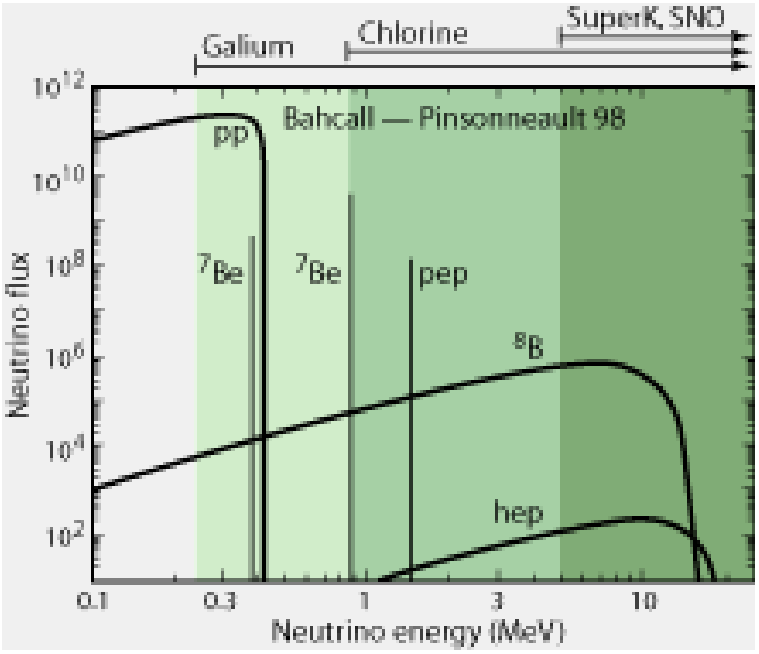

Figure 1: The Standard Solar Model prediction of the solar neutrino flux. Thresholds for each of the solar experiments is shown at the top. SuperK and SNO are only sensitive to Boron-8 and hep neutrinos. The gallium experiments have the lowest threshold and can observe pp neutrinos.

Homestake

Ray Davis' Homestake experiment was the first neutrino experiment designed to look for solar neutrinos. It started in 1965, and after several years of running produced a result for the average capture rate of solar neutrinos of 2.56 ± 0.25 SNU (remember that 1 SNU $= 10^{-36}$ neutrino interactions per target atom per second). The big surprise was that the Standard Solar Models of the time predicted that Homestake should have seen about 8.1 ± 1.2 SNU, over three times larger than the measured rate. This discrepancy became known as **the Solar Neutrino Problem**.

At the time it was assumed that something was wrong with the experiment. After all, the Homestake experiment is based on counting very low rate interactions. How did they know that they were seeing solar neutrinos at all? They had no directional or energy information. The objections towards the experiment became harder to maintain when the Super-Kamiokande results were released.

Super-Kamiokande

The main mode of solar neutrino detection in Super-Kamiokande is the elastic scattering channel $\nu_e + e^- \rightarrow \nu_e + e^-$ which has a threshold of 5 MeV. This threshold comes from the design of the detector - neutrinos with energies less than 5 MeV which elastically scatter in the water will not generate an electron with enough momentum to be seen in the detector. Super-Kamiokande observed a capture rate of about 0.45 ± 0.02 SNU, with a model prediction of 1.0 ± 0.2 SNU, almost a factor of two larger than observation. In addition, since Super-Kamiokande was able to reconstruct the direction of the incoming electron (with some large resolution due to both scattering kinematics - Super-Kamiokande sees the final state electron which isn't quite collinear with the incoming neutrino direction - and to multiple scattering of the final state electron - which smears the directional resolution out even more), it was able to show that the electron neutrinos do indeed come from the sun (see Figure 2).

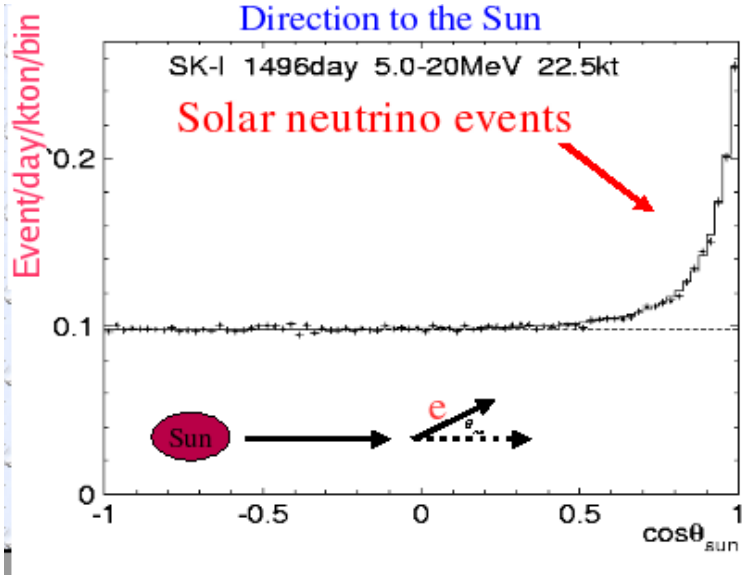

Figure 2: The cosine of the angle between the measured electron in the Super-Kamiokande solar neutrino data, and the direction to the sun at the time the event occurred. A clear peak can be seen for $cos\theta > 0.5$ above an essentially flat background. The peak is broad because of kinematic smearing and multiple scattering of the final state electron in the water.

SAGE and GALLEX

An obvious drawback of both the Chlorine and the water experiments was that they were only sensitive to the relatively rare ^8B and pep neutrinos.The Gallium experiments were able to observe part of the bulk pp neutrino flux. SAGE, which ran with 50 tonnes of Gallium, observed a capture rate of 70.8 ± 5.0 SNU compared to a model prediction of 129 ± 9 SNU. It's counterpart, GALLEX, observed a rate of 77.5 ± 8 SNU. Again the observations were lower than the prediction - this time by about 40%. This is, in itself, important as it shows that deficit is energy dependent.

A summary of these results is shown in Figure 3.

In all experiments, the model seems to overestimate the solar neutrino capture rate by approximately a factor of two although, crucially, the discrepancy appears to be energy dependent - the lower in energy the experiment is able to probe, the less the discrepancy. Such a discrepancy has two main

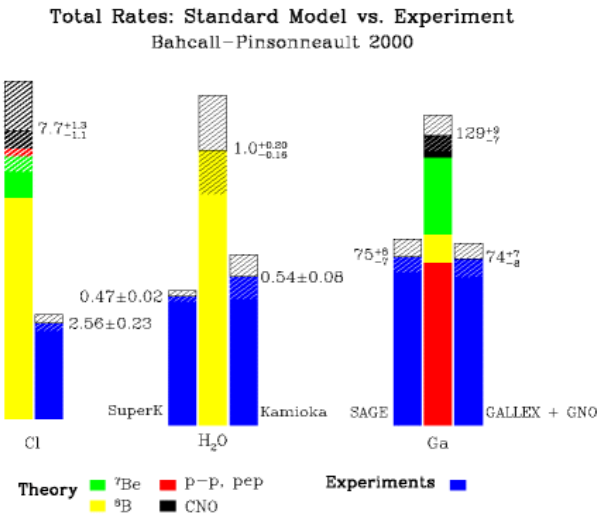

Figure 3: The state of the solar neutrino problem before SNO. Each group of bars represents a different type of experiment : Chlorine on the left, water in the middle and Gallium on the right. The blue bars in each cluster represent the measurements of individual experiments, in SNUs. The middle bar shows the Standard Solar Model prediction. In all cases, the measurements are less than predicted.

solutions. One is that our model of the Sun is just wrong, and the other is that there is something wrong with the neutrinos coming from the sun.

It is now believed that Bahcall's Standard Solar Model (SSM) describes the sun well. This is largely on the basis of data obtained from studies of *helioseismology* - or sun quakes. Helioseismology utilizes waves that propagate throughout the Sun to measure the invisible internal structure and dynamics of a star. There are millions of distinct, resonating, sound waves, seen by the doppler shifting of light emitted at the Sun's surface. The periods of these waves depend on their propagation speeds and the depths of their resonant cavities, and the large number of resonant modes, with different cavities, allows us to construct extremely narrow probes of the temperature, chemical composition, and motions from just below the surface down to the very core of the Sun. The SSM predicts the velocity of sound waves in the Sun as a function of radial distance out from the core. This is shown in Figure 4. The model agrees with measured data to better than 1.0%. Since these sound speeds depend very much on the chemical composition and structure of the star, which are predictions from the SSM, the model is regarded as reliable. Certainly there is no way that one could tweak the model to remove up to 50% of the neutrino output whilst leaving all other observables unaffected.

In order to show that neutrino flavour oscillations are the cause of the Solar Neutrino Problem, it is necessary to be able to observe the solar flux in a way that is independent of neutrino flavour. All solar experiments detect solar neutrinos through charged current interactions in the detector : $\nu_e + X \rightarrow e^- + Y$. The radiochemical experiments used the charged current interaction to generate the unstable ion, whereas the water Cerenkov experiments needed the final state electron as a tag that a ν_e had interacted in the detector. This immediately creates a problem - solar neutrino energies are less than about 30 MeV, whereas the charged muon mass is 105 MeV. In order to interact via the charged current there must be sufficient energy available to create the charged leptons. From the point of view of all the solar experiments, electron neutrinos might well be changing to muon or tau

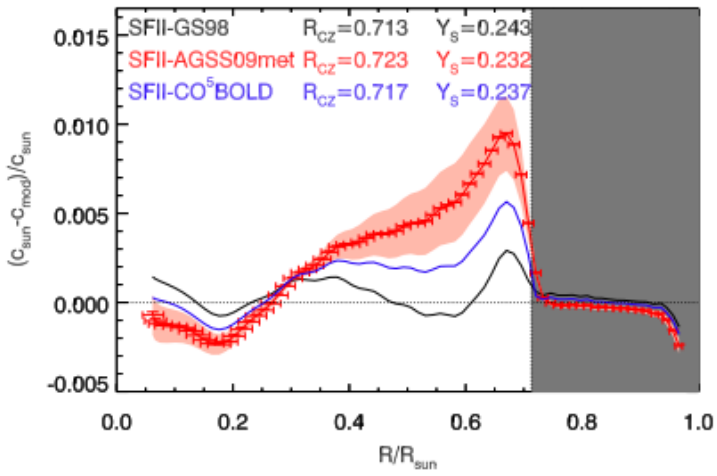

Figure 4: The speed of sound waves in the Sun as a function of radial distance from the solar core for a set of models of solar composition. The graph shows the fractional difference of the SSM from helioseismological data (Serenelli, arXiv:1601.07179 [astro-ph.SR]). Regardless of choice, the model deviates from measurement by less than 1%.

neutrinos, but as there is not enough energy to create the respective charged lepton, and as all the experiments relied on that charged current interaction to detect the neutrino, all experiments just wouldn't be able to see the ν_μ or ν_τ part of the flux. What was needed was a way to measure the total neutrino flux, regardless of flavour. This was finally provided by the SNO detector.

The SNO experiment used a tank of heavy water as its target. Heavy water consists of D_2O with the deuteron containing a proton and a neutron, rather than just a proton (as in Hydrogen). The important point is that the deuteron is a very fragile nucleus. It only takes about 2 MeV to break it apart into a proton and a neutron. Solar neutrinos have energies up to 30 MeV and so any of the neutrino ν_e, ν_μ or ν_τ can break apart a deuteron in a neutral current interaction. SNO was able to detect the final state neutron and so all those neutrinos that weren't visible to the radiochemical or water Cerenkov experiments *are* visible to SNO. In fact, SNO was able to detect neutrino via three different, and redundant, interactions:

- The Elastic Scattering (ES) channel :

$$\nu + e^- \rightarrow \nu + e^- \tag{5}$$

  This is the same sort of interaction used by Super–Kamiokande. Electron neutrinos can, however, interact via both the charged and neutral currents (draw some Feynman diagrams to convince yourself of this), whereas ν_μ and ν_τ neutrinos interact only via the neutral current at these energies (due to the final lepton mass threshold). Elastic scattering probes a combination of the electron, muon and tau neutrino flux given by

$$\phi(\nu_e) + 0.15(\phi(\nu_\mu) + \phi(\nu_\tau)) \tag{6}$$

- The Charged Current (CC) channel :

$$\nu_e + d \rightarrow p + p + e^- \tag{7}$$

This reaction can only be initiated by electron neutrinos and therefore only measure $\phi(\nu_e)$. SNO used this channel to ensure that it was seeing the same reduction in ν_e rate as observed in previous solar neutrino experiments.

- The Neutral Current (NC) channel :

$$\nu + d \rightarrow n + p + \nu \tag{8}$$

This is the important reaction. It measure the total flux : $\phi(\nu_e)+\phi(\nu_\mu)+\phi(\nu_\tau)$. The experimental challenge is to measure that final state neutron. SNO did this 3 different ways as cross checks on their final result.

Using the measurement of the three independent reaction channels, SNO was able to disentangle the individual fluxes of neutrinos. Their measurement of the neutrino fluxes was, in units of $10^{-8} cm^{-2} s^{-1}$,

$$\begin{aligned} \phi_{CC} &= \phi(\nu_e) &&= 1.76 \pm 0.01 \\ \phi_{ES} &= \phi(\nu_e) + 0.15(\phi(\nu_\mu) + \phi(\nu_\tau)) &&= 2.39 \pm 0.26 \\ \phi_{NC} &= \phi(\nu_e) + \phi(\nu_\mu) + \phi(\nu_\tau) &&= 5.09 \pm 0.63 \end{aligned}$$

The numbers are striking. The total flux of muon and tau neutrinos from the Sun $(\phi(\nu_\mu) + \phi(\nu_\tau))$ is $(3.33 \pm 0.63) \times 10^{-8} \mathrm{cm}^{-2} \mathrm{s}^{-1}$, roughly 3 times *larger* than the flux of ν_e. Since we know the Sun only produces electron neutrinos, the only conclusion we can draw is that neutrinos must change flavour between the Sun and the Earth. Furthur, the SSM predicts a total flux of neutrinos with energies greater than 2 MeV (the deuteron break-up energy) of

$$\phi_{SSM} = (5.05 \pm 1.01) \times 10^{-8} \mathrm{cm}^{-2} \mathrm{s}^{-1} \tag{9}$$

which is in very good agreement with the NC flux measured by SNO. Here endeth the Solar Neutrino Problem. Previous experiments *were* seeing less electron neutrino than predicted, because two-thirds of the electron neutrinos were changing flavour on the way from the sun to the earth. The total flux is predicted well by the SSM.

3.1.1 What you should know

- What the solar neutrino problem was, including the specific experiments that were involved (Homestake, Gallex, Super–Kamiokande, SNO)
- Why neither the solar model, or details of the specific experiment could account for the solar neutrino problem, and why the phenomenon of neutrino flavour oscillation could.
- How SNO definitively solved the solar neutrino problem

3.2 Atmospheric Neutrinos and the Atmospheric Neutrino Anomaly

The atmosphere is constantly being bombarded by cosmic rays. These are composed of protons (95%), alpha particles (5%) and heavier nuclei and electrons (< 1%). When the primary cosmic rays hit nuclei in the atmosphere they *shower*, setting up a cascade of hadrons. The atmospheric neutrinos stem from the decay of these hadrons during flight. The dominant part of the decay chain is

$$\pi^+ \to \mu^+ \nu_\mu \quad \mu^+ \to e^+ \nu_e \overline{\nu_\mu} \tag{10}$$

$$\pi^- \to \mu^- \overline{\nu_\mu} \quad \mu^- \to e^- \overline{\nu_e} \nu_\mu \tag{11}$$

At higher energies, one also begins to see neutrinos from kaon decay as well. In general the spectrum of these neutrinos peaks at 1 GeV and extends up to hundreds of GeV. At moderate energies one can see that the ratio

$$R = \frac{(\nu_\mu + \overline{\nu_\mu})}{(\nu_e + \overline{\nu_e})} \tag{12}$$

should be equal to 2. In fact, computer models of the entire cascade process predict this ratio to be equal to 2 with a 5% uncertainty. The total flux of atmospheric neutrinos, however, has an uncertainty of about 20% due to various assumptions in the models.

A detector looking at atmospheric neutrinos is, necessarily, positioned on (or just below) the Earth's surface (see Figure 5). Flight distances for neutrinos detected in these experiments can thus vary from 15 km for neutrinos coming down from an interaction above the detector, to more than 13,000 km for neutrinos coming from interactions in the atmosphere below the detector on the other side of the planet.

3.2.1 Atmospheric Neutrino Detectors and the Atmospheric Neutrino Anomaly

There have been effectively two categories of detectors used to study atmospheric neutrinos - water Cerenkov detectors and tracking calorimeters. Of the former, the most influential has been Super-Kamiokande (again). We will not discuss the latter.

Atmospheric neutrino experiments measure two quantities : the ratio of ν_μ to ν_e observed in the flux, and zenith angle distribution of the neutrinos (that is, the path length distribution). To help interpret the results and to cancel systematic uncertainties most experiments report a *double ratio*

$$R = \frac{(N_\mu/N_e)_{DATA}}{(N_\mu/N_e)_{SIM}} \tag{13}$$

where N_μ is the number of ν_μ events which interacted in the detector (called "muon-like") and N_e is the number of ν_e events which interacted (called "electron-like"). The ratio of $\frac{N_\mu}{N_e}$ is measured in the data and is also measured in a computational model of the experiment, which incorporates all known physics of atmospheric neutrino production, neutrino propagation to the detector and detector response. The absolute flux predictions largely cancel in this double ratio. If the observed flavour composition agrees with expectation that $R = 1$.

A compilation of R values from a number of different experiments is shown in Table 1. With the exception of Frejus, all measurements of R are significantly less than 1, indicating that either there was less ν_μ in the data than in the prediction, or there was more ν_e, or both. This became known as the **Atmospheric Neutrino Anomaly**.

In addition to low values of R, Super-Kamiokande was able to measure the direction of the incoming neutrinos. Neutrinos are produced everywhere in the atmosphere and can reach the detector from all

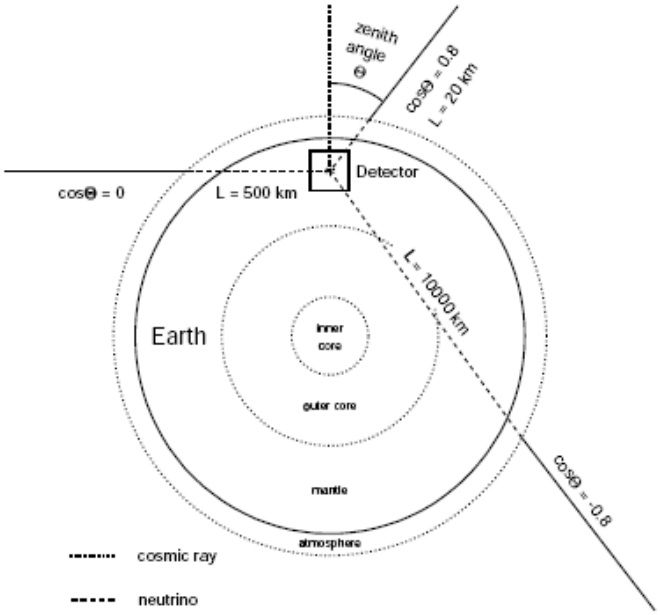

Figure 5: A diagram of an atmospheric neutrino experiment. A detector near the surface sees neutrinos that travel about 15 km looking up, while neutrinos arriving at the detector from below can travel up to 13,000 km. This distance is measured by the "zenith angle"; the polar angle as measured from the vertical direction at the detector : $cos\theta_{zen} = 1$ is for neutrinos coming directly down, whereas $cos\theta_{zen} = -1$ describes upwards-going neutrinos.

directions. In principle, we expect the flux of neutrinos to be isotropic - the same number coming down as going up. The zenith angle distributions from Super-Kamiokande are shown in Figure 6. In this figure, the left column shows the ν_e ("e-like") events, where as the right column depicts ν_μ events. The top and middle rows show low energy events where the neutrino energy was less than 1 GeV, whilst the bottom row shows events where the neutrino energy was greater than 1 GeV. The red line shows what should be expected from standard cosmic ray models and the black points show what Super-Kamiokande actually measured. Clearly, whilst the electron-like data agrees reasonably well with expectation, the muon-like data deviates significantly. At low energies appoximately half of the ν_μ are missing over the full range of zenith angles. At high energy the number of ν_μ coming down from above the detector seems to agree with expectation, but half of the same ν_μ coming up from below the detector are missing.

Experiment	Type of experiment	R
Super-Kamiokande	Water Cerenkov	0.675 ± 0.085
Soudan2	Iron Tracking Calorimeter	0.69 ± 0.13
IMB	Water Cerenkov	0.54 ± 0.12
Kamiokande	Water Cerenkov	0.60 ± 0.07
Frejus	Iron Tracking Calorimeter	1.0 ± 0.15

Table 1: Measurements of the double ratio for various atmospheric neutrino experiments.

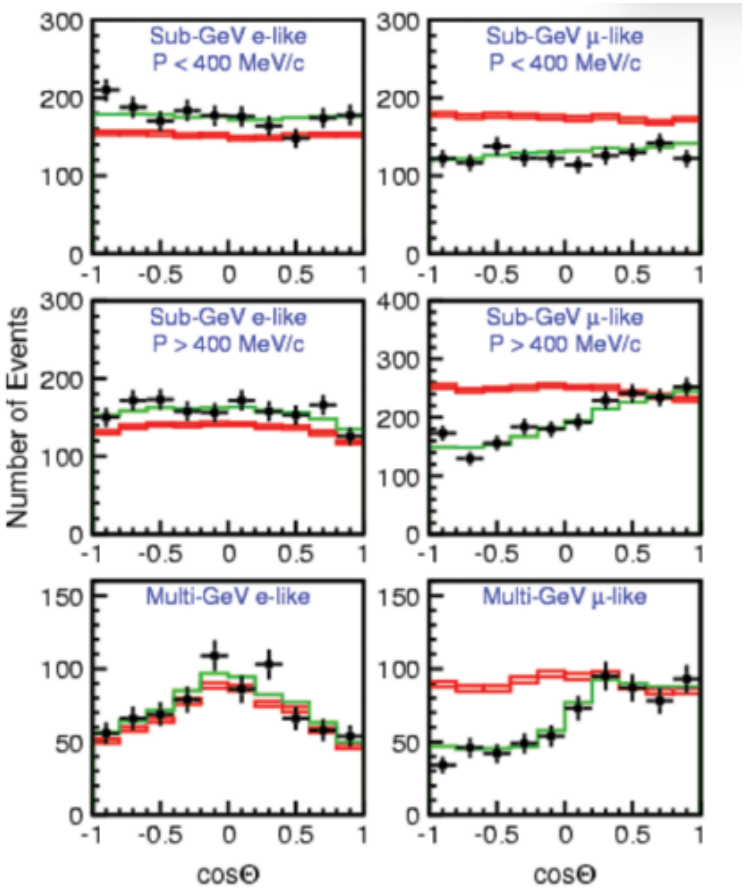

Figure 6: Zenith angle distributions of ν_μ and ν_e-initiated atmospheric neutrino events detected by Super-Kamiokande. The left column shows the ν_e ("e-like") events, where as the right column depicts ν_μ events. The top and middle rows show low energy events where the neutrino energy was less than 1 GeV, whilst the bottom row shows events where the neutrino energy was greater than 1 GeV. The red line shows what should be expected from standard cosmic ray models and the black points show what Super-Kamiokande actually measured.

These results are reasonably easy to explain within the context of flavour oscillations. Neutrinos arriving at the Super-Kamiokande detector at different zenith angles have travelled anywhere from 15 km (for neutrinos coming straight down) to 13000 km (for neutrinos coming straight up). Referring back to the oscillation probability in Equation 4, we see that if $\Delta m^2 \sim 10^{-3}\text{eV}^2$ and the neutrino energy is about 10 GeV, then for neutrinos coming down the oscillation probability will be roughly zero, whereas for neutrinos coming up, the oscillation probability will be roughly $\frac{1}{2}\sin^2(2\theta)$ (where the factor of 0.5 comes from averaging the kinematic factor, $sin^2(1.27\Delta m^2 L/E)$, over many oscillation periods). Furthur, the fact that ν_μ neutrinos are reduced, but the electron neutrinos are not enhanced suggests that the dominant oscillation mode for the atmospheric neutrinos is $\nu_\mu \rightarrow \nu_\tau$. Unfortunately Super-Kamiokande cannot easily detect ν_τ interactions and can't check this option itself.

Both the solar and atmospheric neutrino problems can be explained by neutrino flavour oscillations. Let's look a bit more rigorously at this phenomenon. We will first do this assuming that only 2 neutrino flavours exist - say ν_e and ν_μ, and then we will generalise to the 3-neutrino case.

3.2.2 What you should know

- What the atmospheric neutrino anomaly was, including the double ratio and the zenith angle dependencies of the muon and electron neutrino flux from cosmic ray showers.
- How neutrino flavour oscillations can be used to predict such zenith angle and energy dependencies.
- How the data from Super–Kamiokande showed that the atmospheric neutrino anomaly could be interpreted in the context of neutrino flavour oscillations.

4 Two Flavour Neutrino Oscillation Theory

Note: You should be able to reproduce the two flavour oscillation probability derivation

The ground rules are : the eigenstates of the Hamiltonian are $|\nu_1>$ and $|\nu_2>$ with eigenvalues m_1 and m_2 for neutrinos at rest. A neutrino of type j with momentum p is an energy (or mass) eigenstate with eigenvalues $E_j = \sqrt{m_j^2 + p^2}$. Neutrinos are produced in weak interactions in weak eigenstates of definite lepton number ($|\nu_e>$, $|\nu_\mu>$ or $|\nu_\tau>$) that are *not* energy eigenstates. These two sets of states are related to each other by a unitary matrix. which we can write as U where, in two dimensions,

$$U = \begin{pmatrix} U_{\alpha 1} & U_{\alpha 2} \\ U_{\beta 1} & U_{\beta 2} \end{pmatrix} \tag{14}$$

Suppose that we generate a neutrino beam with some amount of neutrino flavours ν_e and ν_μ. Then in terms of the mass states ν_1 and ν_2 we can write

$$\begin{pmatrix} |\nu_e> \\ |\nu_\mu> \end{pmatrix} = U \begin{pmatrix} |\nu_1> \\ |\nu_2> \end{pmatrix} = \begin{pmatrix} U_{\alpha 1} & U_{\alpha 2} \\ U_{\beta 1} & U_{\beta 2} \end{pmatrix} \begin{pmatrix} |\nu_1> \\ |\nu_2> \end{pmatrix} \tag{15}$$

More compactly we can write the flavour state ν_α as a linear combination,

$$|\nu_\alpha> = \sum_{k=1,2} U_{\alpha k} |\nu_k> \tag{16}$$

Suppose we generate a neutrino beam containing a flavour state $|\nu_\alpha(0,0)>$ which describes a neutrino generated with a definite flavour α at space-time point $(x,t)=(0,0)$. Suppose we aim the neutrinos along the x-axis and let them propagate in a free space towards a detector some distance L away.

The $\nu_{1,2}$ propagate according to the time-dependent Schrodinger Equation with no potentials

$$i\frac{\partial}{\partial t}|\nu_i(x,t)>=E|\nu_i(x,t)>=-\frac{1}{2m_i}\frac{\partial^2}{\partial x^2}|\nu_i(x,t)> \quad i\exists 1,2 \tag{17}$$

The solution to this equation is a plane-wave :

$$|\nu_k(x,t)>=e^{-i(E_kt-p_kx)}|\nu_k(0,0)>=e^{-i\phi_k}|\nu_k(0,0)> \tag{18}$$

where $p_k=(t,\mathbf{p})$ is the 4-momentum of the neutrino mass state $|\nu_k>$ and $x=(t,\mathbf{x})$ is the 4-space vector.

At some later space-time point (x,t) then the flavour state α will be

$$|\nu_\alpha(x,t)>=\sum_{k=1,2}U_{\alpha k}|\nu_k(x,t)>=\sum_{k=1,2}U_{\alpha k}e^{-i\phi_k}|\nu_k(0,0)> \tag{19}$$

Inverting the mixing matrix we can write

$$|\nu_k(0,0)>=\sum_\gamma U^*_{\gamma k}|\nu_\gamma(0,0)> \tag{20}$$

Substituting Equation 20 into Equation 19 we then write the flavour state $|\nu_\alpha>$ at space-time point (x,t) in terms of the flavour states at the generation point

$$|\nu_\alpha(x,t)>=\sum_{k=1,2}U_{\alpha k}e^{-i\phi_k}\sum_\gamma U^*_{\gamma k}|\nu_\gamma(0,0)>=\sum_\gamma\sum_k U^*_{\gamma k}e^{-i\phi_k}U_{\alpha k}|\nu_\gamma(0,0)> \tag{21}$$

and so the transition amplitude for detecting a neutrino of flavour β at space-time point (t,x) given that we generated a neutrino of flavour α at space-time point $(0,0)$ is

$$\begin{aligned}A(\nu_\alpha(0,0)\to\nu_\beta(x,t)) &= <\nu_\beta(x,t)|\nu_\alpha(0,0)> \\ &= \sum_\gamma\sum_k U_{\gamma k}e^{i\phi_k}U^*_{\beta k}<\nu_\gamma(0,0)|\nu_\alpha(0,0)> \\ &= \sum_k U_{\alpha k}e^{i\phi_k}U^*_{\beta k}\end{aligned}$$

where the last step comes from the orthogonality of the flavour states, $<\nu_\gamma(0,0)|\nu_\alpha(0,0)>=\delta_{\gamma\alpha}$.

The oscillation probability is the coherent sum

$$\begin{aligned}P(\nu_\beta\to\nu_\alpha)=|A(\nu_\beta(0,0)\to\nu_\alpha(x,t))|^2 &= |\sum_k U_{\alpha k}e^{i\phi_k}U^*_{\beta k}|^2 \\ &= \sum_k U_{\alpha k}e^{i\phi_k}U^*_{\beta k}\sum_j U^*_{\alpha j}e^{-i\phi_j}U_{\beta j} \\ &= \sum_j\sum_k U_{\alpha k}U^*_{\beta k}U^*_{\alpha j}U_{\beta j}e^{-i(\phi_j-\phi_k)}\end{aligned}$$

In the case of 2-dimensions, there is only one unitary matrix - the 2x2 rotation matrix which which rotates a vector in the flavour basis into a vector in the mass basis :

$$U = \begin{pmatrix} cos\theta & sin\theta \\ -sin\theta & cos\theta \end{pmatrix}$$

so that

$$\begin{pmatrix} \nu_\alpha \\ \nu_\beta \end{pmatrix} = \begin{pmatrix} cos\theta & sin\theta \\ -sin\theta & cos\theta \end{pmatrix} \begin{pmatrix} \nu_1 \\ \nu_2 \end{pmatrix}$$

where θ is an unspecified parameter known as the *mixing angle*. This will have to be measured by an experiment. Using this matrix, we can find work out the oscillation probability in a somewhat more transparent form. The sum is over 4 elements with combinations of $k\exists(1,2)$ and $j\exists(1,2)$:

- (k=1,j=1) : $U_{\alpha 1}U^*_{\beta 1}U^*_{\alpha 1}U_{\beta 1}e^{-i(\phi_1-\phi_1)} = |U_{\beta 1}|^2|U_{\alpha 1}|^2$
- (k=1, j=2) : $U_{\alpha 1}U^*_{\beta 1}U^*_{\alpha 2}U_{\beta 2}e^{-i(\phi_2-\phi_1)}$
- (k=2, j=1) : $U_{\alpha 2}U^*_{\beta 2}U^*_{\alpha 1}U_{\beta 1}e^{-i(\phi_1-\phi_2)}$
- (k=2, j=2) : $U_{\alpha 2}U^*_{\beta 2}U^*_{\alpha 2}U_{\beta 2}e^{-i(\phi_2-\phi_2)} = |U_{\beta 2}|^2|U_{\alpha 2}|^2$

So the oscillation probability is

$$\begin{aligned} P(\nu_\alpha \to \nu_\beta) &= (|U_{\beta 1}|^2|U_{\alpha 1}|^2 + |U_{\beta 2}|^2|U_{\alpha 2}|^2) + U_{\alpha 1}U^*_{\beta 1}U_{\alpha 2}U^*_{\beta 2}(e^{i(\phi_2-\phi_1)} + e^{-i(\phi_2-\phi_1)}) \\ &= (|U_{\beta 1}|^2|U_{\alpha 1}|^2 + |U_{\beta 2}|^2|U_{\alpha 2}|^2) + 2U_{\alpha 1}U^*_{\beta 1}U_{\alpha 2}U^*_{\beta 2}cos(\phi_2-\phi_1) \\ &= (sin^2\theta cos^2\theta + cos^2\theta sin^2\theta) + 2(cos\theta)(-sin\theta)(sin\theta)(cos\theta)cos(\phi_2-\phi_1) \\ &= 2cos^2\theta sin^2\theta(1-cos(\phi_2-\phi_1)) \\ &= 2sin^2(2\theta)sin^2(\frac{\phi_2-\phi_1}{2}) \end{aligned}$$

where in the last two steps I have used the trigonometric identites $cos\theta sin\theta = \frac{1}{2}sin(2\theta)$ and $2sin^2(\theta) = 1 - cos(2\theta)$.

At this point we need to do something with the phase difference $\phi_2 - \phi_1$. Recall that

$$\phi_i = E_i t - p_i x \tag{22}$$

The phase difference is, then,

$$\phi_2 - \phi_1 = (E_2 - E_1)t - (p_2 - p_1)x \tag{23}$$

If we assume that the neutrinos are relativistic (a reasonable assumption), then $t = x = L$ (where L is the conventional measure of the distance between source and detector) and

$$p_i = \sqrt{E_i^2 - m_i^2} = E_i\sqrt{1 - \frac{m_i^2}{E_i^2}} \approx E_i(1 - \frac{m_i^2}{E_i^2}) \tag{24}$$

so

$$\phi_2 - \phi_1 = (\frac{m_1^2}{2E_1} - \frac{m_2^2}{2E_2})L \tag{25}$$

Now we make a bit of a dodgy approximation. It is usual to assume that the mass eigenstates are created with either the same momentum or the energy. This assumption is not necessary, but we find that whatever assumption is made you get the the same result. The fact that we have to make such an approximation comes from the way that we are modelling the mass eigenstates as plane waves. If we were to do the analysis assuming that the mass states were wavepackets instead we would (i) not need the equal momentum (equal energy) assumption and (ii) would still get the same answer. So, let's assume that the energies of the mass states are identical. Then

$$\phi_2 - \phi_1 = (\frac{m_1^2}{2E_1} - \frac{m_2^2}{2E_2})L = \frac{\Delta m^2 L}{2E} \tag{26}$$

where $\Delta m^2 = m_1^2 - m_2^2$ and $E_1 = E_2 = E$.

Substituting back into the probability equation we get

$$P(\nu_\alpha \to \nu_\beta) = sin^2(2\theta) sin^2(\frac{\Delta m^2 L}{4E_\nu}) \tag{27}$$

and if we agree to measure L in units of kilometres and E in units of GeV and pay attention to all the $\hbar$ and c we've left out we end up with

$$P(\nu_\alpha \to \nu_\beta) = sin^2(2\theta) sin^2(1.27\Delta m^2 \frac{L}{E_\nu}) \tag{28}$$

This is the probability that one generates a ν_α but detects ν_β and is called the oscillation probability. The corresponding survival probability is the chance of generating a ν_α and detecting a ν_α : $P(\nu_\alpha \to \nu_\alpha) = 1 - P(\nu_\alpha \to \nu_\beta)$ in the two-flavour approximation.

As you can see, the oscillatory behaviour comes from the difference in the energy eigenvalues of $|\nu_1>$ and $|\nu_2>$ $(E_2 - E_1)$, which we interpret as coming from different masses for each of the mass eigenvalues.

A plot of this function is shown in Figure 7 for a particular set of parameters : $\Delta m^2 = 3 \times 10^{-3} eV^2$, $sin^2(2\theta) = 0.8$ and $E_\nu = 1$GeV. At $L = 0$, the oscillation probability is zero and the corresponding survival probability is one. As L increases the oscillations switch on and the oscillation probability increases until $1.27\Delta m^2 \frac{L}{E} = \frac{\pi}{2}$ or $L = 400$ km. At this point the oscillation is a maximum. However, the mixing angle is just $sin^2(2\theta) = 0.8$ so at maximal mixing, only 80% of the initial neutrinos have oscillated away. As L increases furthur, the oscillation dies down until, around $L = 820$ km, the beam is entirely composed of the initial neutrino flavour. If $sin^2(2\theta) = 1.0$, the oscillations would be referred to as *maximal*, meaning that at some point on the path to the detector 100% of the neutrinos have oscillated.

As a side comment, the derivation of the oscillation probability depends on two assumptions : that the neutrino flavour and mass states are mixed and that we create a coherent superposition of mass states at the weak vertex. This coherent superposition reflects the fact that we can't experimentally resolve which mass state was created at the vertex. One might ask oneself what we would expect to see if we *did* know which mass state was created at the vertex. If we knew that, we would know the mass of the neutrino state that propagates to the detector. There would be no superposition, no phase difference and no flavour oscillation. However there *would* be flavour change. Suppose that at the vertex we create a lepton of flavour α and a specific mass state, $|\nu_k>$. Mixing implies that we've picked out the k^{th} mass state from the α flavour state. The probability of doing this is just

$$|<\nu_k|\nu_\alpha>|^2 = U_{k\alpha}^2 \tag{29}$$

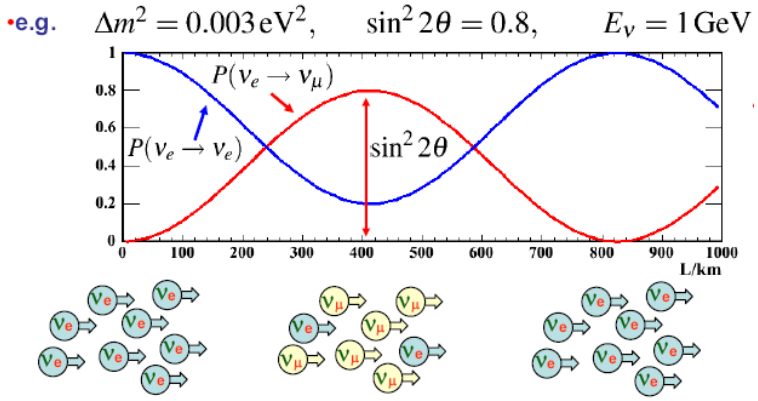

Figure 7: The oscillation probability as a function of the baseline, L, for a given set of parameters : $\Delta m^2 = 3 \times 10^{-3} eV^2$, $sin^2(2\theta) = 0.8$ and $E_\nu = 1$GeV (Figure taken from Prof. Mark Thomson's Particle Physics lecture notes).

This mass state then propagates to the detector, and is detected as a neutrino of flavour β with probability $| < \nu_\beta | \nu_k > |^2 = |U_{\beta k}|^2$. The flavour change probability is then the *incoherent* sum

$$P(\nu_\alpha \to \nu_\beta)^{mixing} = \sum_k | < \nu_\beta | \nu_k > e^{-i\phi_k} < \nu_k | \nu_\alpha > |^2 = \sum_k |U_{\alpha k}|^2 |U_{\beta k}|^2 \tag{30}$$

In the two-flavour approximation, we would have a ν_e flavour transition probability of

$$\begin{aligned} P(\nu_e \to \nu_\mu) &= |U_{e1}|^2 |U_{\mu 1}|^2 + |U_{e2}|^2 |U_{\mu 2}|^2 && (31) \\ &= 2cos^2\theta sin^2\theta && (32) \\ &= \frac{1}{2} sin^2(2\theta) && (33) \\ & && (34) \end{aligned}$$

and a survival probability of $P(\nu_e \to \nu e) = 1 - \frac{1}{2} sin^2 2\theta$. In conclusion, if the mass states and flavour states are mixed then will always be a probability of flavour change. If we can resolve the mass states at the production vertex, however, this probability will *not* oscillate. That is, it will be the same where ever you put the detector. The oscillation only occurs when you don't know what mass state was produced (which, realistically, is true all of the time in the case of the neutrino mass states) and is a purely quantum mechanical effect.

4.1 What you should know

- How to derive the two-flavour neutrino oscillation formula, including an understanding of the approximations that are usually made.

5 Interpretation of the Atmospheric Neutrino Problem

Look again at Figure 6. How can we interpret this data in terms of oscillations?

Consider the left hand column first. This shows the zenith angle dependence of electron-like data in different energy bins. This column correlates with the ν_e component of the cosmic ray neutrino flux. Notice that there is very little difference between the data and the model prediction in the absence of oscillations (red line). This suggests that, if neutrino oscillations are responsible for the atmospheric neutrino problem, they do not involve the ν_e component (or, at the very least, the ν_e oscillation mode is suppressed). Hence we can assume that the oscillations are largely $\nu_\mu \rightarrow \nu_\tau$.

Now consider the bottom right hand plot in Figure 6. This shows the zenith angle dependence of high energy muon-like data, which correlates with the ν_μ component of the cosmic ray flux. For neutrinos coming directly from above ($cos\theta_{zen} = 1$) there is no difference between data and the expected distribution in the absence of oscillations. As the zenith angle increases towards and through 90 degrees, the discrepancy between data and expectation grows until, for neutrinos coming upwards ($cos\theta_{zen} = -1$) there is a discrepancy of about 50%. The two-flavour oscillation equation is

$$P(\nu_\mu \rightarrow \nu_\tau) = sin^2(2\theta_{atm})sin^2(1.27\Delta m^2_{atm}\frac{L}{E_\nu}) \tag{35}$$

where θ_{atm} and Δm^2_{atm} are the mixing angle and squared mass difference for the atmospheric neutrinos respectively. Let us suppose that Δm^2_{atm} is around $1 \times 10^{-3} eV^2$. If L/E is small, then $sin^2(1.27\Delta m^2_{atm}\frac{L}{E_\nu})$ is too small for the oscillations to have started. Suppose that the multi-GeV plot has neutrino energy of about 1 GeV. The baseline for downward going neutrino is on the order of 10 km, so

$$1.27\Delta m^2_{atm}\frac{L}{E_\nu} = 1.27 \times 10^{-3} \times 10(km)/1(GeV) = 0.00127 \tag{36}$$

Hence $P(\nu_\mu \rightarrow \nu_\tau) = sin^2(2\theta_{atm})sin^2(0.00127) <= sin^2(0.00127) = 1.6 \times 10^{-6}$. This can explain the downward going muon-like behaviour - the baseline isn't long enough for the relevant oscillations to have started. However, as the zenith angle sweeps around from zero degrees to 180 degrees, the distance neutrinos travel to the detector (see Figure 5) sweeps from around 10 km all the way to around 13000 km. At a baseline of 13000 km,

$$1.27\Delta m^2_{atm}\frac{L}{E_\nu} = 1.27 \times 10^{-3} \times 13000(km)/1(GeV) = 16.51 \tag{37}$$

Here $P(\nu_\mu \rightarrow \nu_\tau) = sin^2(2\theta_{atm})sin^2(16.51) <= sin^2(16.51) = 0.51$. This explains the upward-going muon behaviour. About 50% have oscillated away which seems to agree with the data. In this case the frequency of oscillation is so fast that the $sin^2(1.27\Delta m^2_{atm}\frac{L}{E_\nu})$ term just averages to 0.5 and so, $P(\nu_\mu \rightarrow \nu_\tau) \approx 0.5sin^(2\theta_{atm})$. This also seems to suggest that $sin^(2\theta_{atm}) \approx 1.0$ or that the mixing angle is 45 degrees.

In fact, after proper analysis we find that

$$\Delta m^2_{atm} = 3 \times 10^{-3}\text{eV}^2 \qquad sin^2(2\theta_{atm}) = 1.0 \tag{38}$$

and that the oscillation is almost completely $\nu_\mu \rightarrow \nu_\tau$.

5.1 Accelerator Verification

As scientists we must be able to reproduce a measurement. We use accelerator experiments to check the atmospheric neutrino results. Why accelerators? Well, we need to find an L/E combination which matches a Δm^2 of 0.003 eV^2. Accelerator neutrinos have energies on the order of 1 GeV, so the optimum baseline is about 400 km, which is experimentally doable.

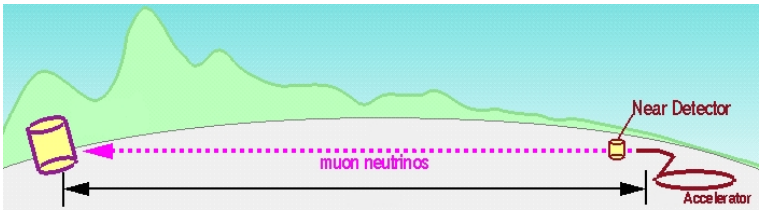

Figure 8: A schematic of a long-baseline neutrino oscillation experiment.

A schematic of a *long-baseline* experiment is shown in Figure 8. The beam is pointed at a detector a few hundred kilometers away. This detector has to be large, in order to detect a large enough number of neutrinos to make a reasonably precise analysis. This detector is generally called the *Far Detector*. A detector, called the *Near Detector*, is usually also built near the beam production point. This is used to measure the neutrino beam before oscillation has happened and should be built of the same kind of technology as the Far Detector to minimise systematic effects.

There are two types of experiments :

- **Disappearance Experiments :** In a disappearance experiment one observes the energy spectrum of a beam of neutrinos at the beam source, before oscillations have started, and at the far detector, after oscillations. The ratio of these spectra should show the oscillation pattern as in Figure 9. This figure shows the ratio of the far detector neutrino energy spectrum to the near detector neutrino energy spectrum. The dip is indicative of neutrinos oscillating away, with the depth of the dip a measure of the mixing angle $sin^2(2\theta)$ and the position of the dip on the energy axis indicative of the relevant Δm^2. The subtlety with this kind of experiment

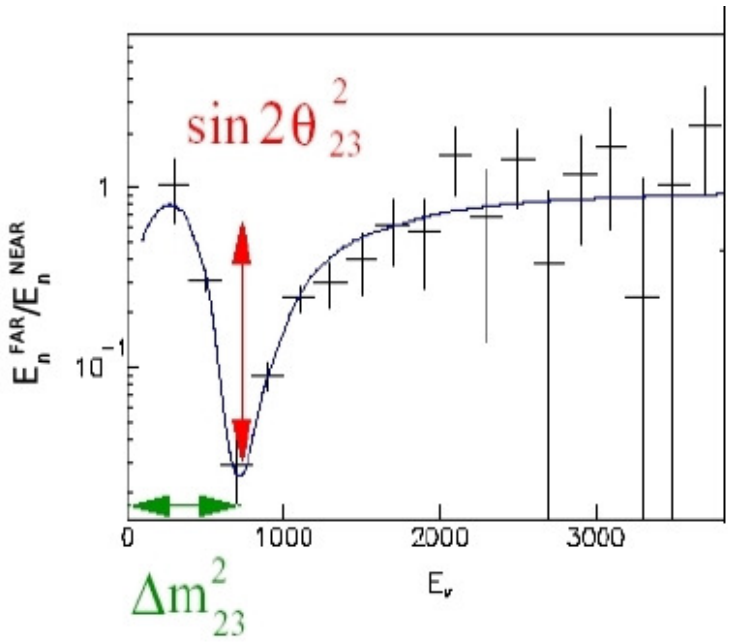

Figure 9: Ratio of neutrino energy spectra before and after oscillation

is in understanding the beam before oscillation happens. This can be a very complicated task

(since, as we know, you never see neutrinos themselves). Getting this wrong could skew the results badly and lead to a mismeasurements of the oscillation parameters.

- **Appearance Experiments :** An appearance experiment looks for the appearance of one flavour of neutrino in a beam that was generated purely of a different flavour. The problems with this type of experiment is understanding any backgrounds in the far detector (or the beam) which could mimic the appearance signature.

5.2 The T2K Experiment

The latest measurements of the atmospheric oscillation parameters has recently been made with the T2K (Tokai-2-Kamioka) experiment in Japan. This is a long-baseline experiment that has been built to measure the θ_{13} mixing angle (see the discussion on the θ_{13} measurements below), but measurements in the 23−sector can also be made with unprecedented precision. T2K directs a 99.5% pure beam of ν_μ neutrinos from the J-PARC facility in a small town on the East Coast of Japan called Tokai. The beam is directed towards the Super-Kamiokande water Cerenkov detector in the mountains off the West Coast of Japan, about 295 km away. The experiment is the first beam to operate off-axis, so that the beam is directed to one side of Super-Kamiokande by about 2.5^o. The neutrino energy spectrum that would be expected at Super-Kamiokande in the absence of oscillations is shown in right plot in Figure 10. The average neutrino energy is about 600 MeV.

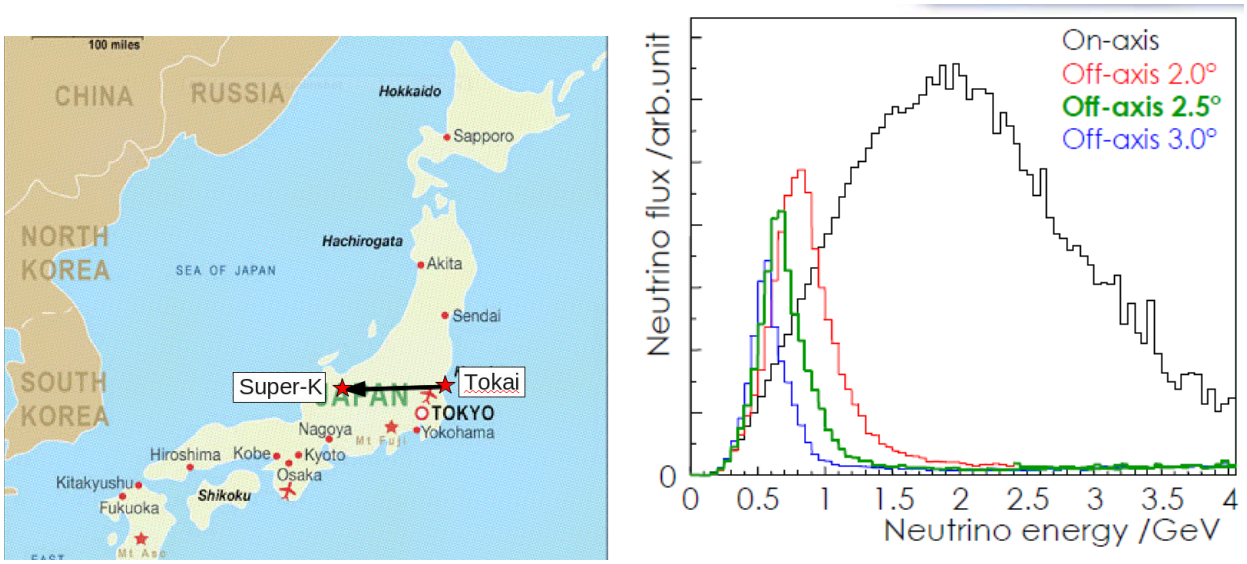

Figure 10: (Left) Baseline of the T2K experiment (Right) Neutrino energy spectrum expected to be seen at Super-Kamiokande in the absence of neutrino oscillations. The black line shows the on-axis spectrum. Super-Kamiokande, though, is about 2.5^o off-axis and will view the much more collimated spectrum delineated by the green line.

The latest ν_μ disappearance measurements are shown in Figure 11. The figure on the left shows the neutrino energy spectrum expected to be seen in the far detector in the absence of oscillations (blue histogram). The data is shown by the black dots. A fit to a three-flavour oscillation model is shown by the red line. The fitted oscillaton contour is shown on the right. The T2K result is

shown by the black-outlined region, the results from two other long-baseline experiments, MINOS[1] and Super-K are shown by the red-outlined region and the blue-outlined regions respectively. T2K now holds the best measurement for the mixing angle and mass difference for the 23−sector. The best fit point is at $(sin^2 2\theta, \Delta m^2)_{best} = (1.0, 2.51 \pm 0.12 \times 10^{-3}\text{eV}^2)$.

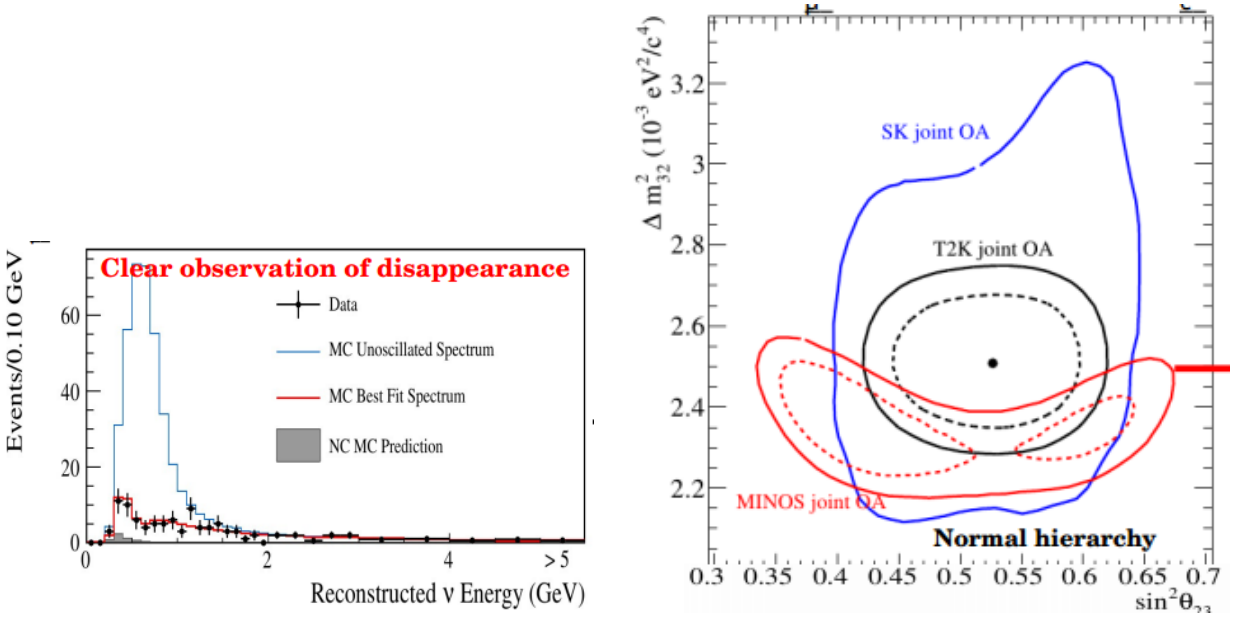

Figure 11: 2015 T2K disappearance data. The figure on the left shows the neutrino energy spectrum expected to be seen in the far detector in the absence of oscillations (blue histogram). The data is shown by the black dots. A fit to a three-flavour oscillation model is shown by the red line. The fitted oscillaton contour is shown on the right. The T2K result is shown by the black line. Results from two other experiments : Super-K and the MINOS long baseline experiment are shown in blue and red respectively.

5.3 Verification that the atmospheric oscillations are mostly $\nu_\mu \to \nu_\tau$

Super-K cannot view ν_τ. It is conceivable that some other mechanism could be responsible for the ν_μ disappearance. What we really need to see is $\nu_\mu \to \nu_\tau$ *appearance*.

An experiment called OPERA, running in the CERN-to-Gran-Sasso (CNGS) beam, was designed to check this assumption. The CNGS beam has an average muon neutrino energy of 17 GeV and the distance from the Gran Sasso lab in Italy to CERN is 732 km. This makes it sensitive to neutrino flavour oscillations with $\Delta m^2 \approx 10^{-3}$ eV^2. OPERA is a tracking experiment using photographic emulsion as it's tracking medium (in much the same way as the DONUT experiment which first discovered the ν_τ in 2000). OPERA is constructed from layers of bricks of interleaved photographic emulsion and lead layers as shown in Figure 12.

[1]MINOS was a long-baseline detector that ran in the NuMI beam at Fermilab from 2005 to 2014. It consisted of two iron-scintillator tracking calorimeters separated by a baseline of 750 km. The far(near) detector used iron plates as the target and massed 5400(980) tonnes interspersed with scintillator to aid particle tracking. Both detectors were magnetised.

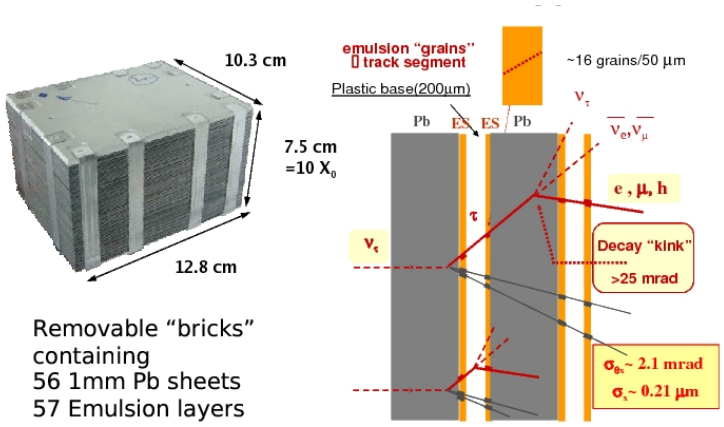

Figure 12: (left) An OPERA brick containing layers of photographic emulsion and lead. (right) the measurement principle. Charged particles from interactions in the lead create short tracks in the photographic emulsion which are measured in off-line scanners. A tau is recognised from the characteristic decay kink.

These bricks are replaceable and are arranged in two target walls separated by scintillator planes. The scintillator planes are used to localise the brick in which a neutrino interaction occurred. Once this vertex brick is known, it is removed from the detector and the photographic emulsion is developed and then scanned by sophisticated off-line image analysers. The interaction characteristics are then measured. A charged-current interaction of a ν_τ generates a short τ track which typically decays hadronically. Figure 13 shows the first ν_τ interaction observed in a brick. The short yellow lines show the track left by each particle as it moves through the photographic emulsion, and the connecting lines show the event reconstruction. The τ is the short red track near the vertex.

To date, OPERA has measured 5 ν_τ interaction with an expected background in the absence of neutrino oscillations of 0.25 events. The oscillation analysis suggests a $\Delta m^2 = 3.3 \times 10^{-3}$ eV^2, consistent with other oscillation experiments. From this we know that the atmospheric oscillation mode is mostly $\nu_\mu \to \nu_\tau$.

5.4 What you should know

- How the atmospheric neutrino data can be interpreted in the context of two-flavour neutrino oscillations.
- What a long–baseline experiment is, and the difference between disappearance and appearance experiments.
- What the T2K experiment was and how it verified the atomspheric oscillation solution.
- You do **not** need to know the details of the OPERA experiment - just what it has been able to show.

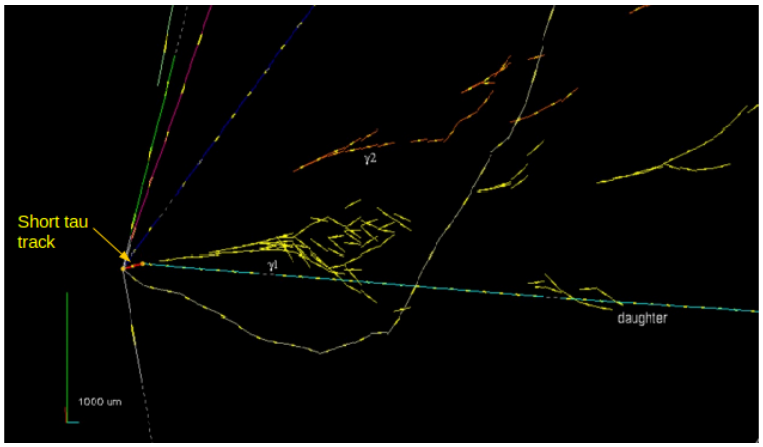

Figure 13: The first ν_τ interaction observed by the OPERA experiment.

6 Interpretation of the Solar Neutrino Data

Naively one might assume that one can do the same sort of analysis as for atmospheric neutrinos. The sun is about $L = 10^8$ km away from the earth, and the neutrino energy is on the order of 10 MeV. That would seem to suggest a Δm^2_{sol} of about 1×10^{-10} eV^2. However, there is something else going on in the sun.

6.1 Matter effects

Note: You should know what matter effects are, and how they influence neutrino oscillations, but you will not be required to reproduce any of the mathematics. The derivations below are included to aid understanding only.

Neutrino oscillations occur because of a difference in phase between the wavepackets of each of the mass eigenstates. This phase difference can occur from wavepackets which propagate with different velocities arising from mass differences. This is what happens in the vacuum. In matter, however, the phase difference is determined by the total energy of the mass eigenstate. If the neutrino is propagating in a potential, V, then the total energy of a state is $E+V$, and if the potential is *different* for different neutrino flavours (i.e. different flavours interact differently) then a phase difference can be introduced through the interaction potential - and the neutrinos will oscillate through matter effects. Let's see how this might work.

Suppose a neutrino is born with momentum p. In the vacuum, the mass states with masses m_i have energies $E_i = \sqrt{p^2 + m_i^2} \approx p + \frac{m_i^2}{2p}$.

The the time dependence of the mass eigenstates has already been written in Equation 18

$$|\nu_i(x,t)> = e^{-i(E_i t - \mathbf{p}\cdot\mathbf{x})}|\nu_i(0,0)> \tag{39}$$

Differentiating this equation with respect to time, and ignoring the common phase factor $e^{i\mathbf{p}\cdot\mathbf{x}}$, we obtain the time development equation, in matrix form,

$$i\frac{d}{dt}\begin{pmatrix}\nu_1\\ \nu_2\end{pmatrix} = H\begin{pmatrix}\nu_1\\ \nu_2\end{pmatrix} \tag{40}$$

where H is the Hamiltonian operator. In a vacuum, this operator is

$$H = \frac{1}{2E}\begin{pmatrix} m_1^2 & 0 \\ 0 & m_2^2 \end{pmatrix} \tag{41}$$

Now, we can write Equation 40 in the flavour states, ν_α and ν_β, assuming the usual 2x2 mixing matrix

$$U = \begin{pmatrix} cos\theta & sin\theta \\ -sin\theta & cos\theta \end{pmatrix} \tag{42}$$

as

$$\begin{pmatrix} \nu_\alpha \\ \nu_\beta \end{pmatrix} = U \begin{pmatrix} \nu_1 \\ \nu_2 \end{pmatrix} \tag{43}$$

Equation 40 may be expressed in the flavour basis as

$$i\frac{d}{dt}\begin{pmatrix} \nu_1 \\ \nu_2 \end{pmatrix} = U^\dagger i\frac{d}{dt}\begin{pmatrix} \nu_\alpha \\ \nu_\beta \end{pmatrix} = H\begin{pmatrix} \nu_1 \\ \nu_2 \end{pmatrix} = HU^\dagger \begin{pmatrix} \nu_\alpha \\ \nu_\beta \end{pmatrix} \tag{44}$$

or, multiplying on the left by U

$$i\frac{d}{dt}\begin{pmatrix} \nu_\alpha \\ \nu_\beta \end{pmatrix} = UHU^\dagger \begin{pmatrix} \nu_\alpha \\ \nu_\beta \end{pmatrix} \tag{45}$$

In the vacuum, the transformed Hamiltonian is (trust me on this....)

$$H_f = UHU^\dagger = \frac{(m_1^2 + m_2^2)}{2E}\mathbf{1} + \frac{\Delta m^2}{2E}\begin{pmatrix} -cos2\theta & sin2\theta \\ sin2\theta & cos2\theta \end{pmatrix} \tag{46}$$

where $\mathbf{1}$ is the 2x2 unit matrix. For convenience, let's label $(\frac{(m_1^2+m_2^2}{4E})\mathbf{1}$ as H_0.

$$i\frac{d}{dt}\begin{pmatrix} \nu_\alpha \\ \nu_\beta \end{pmatrix} = [H_0 + \frac{\Delta m^2}{4E}\begin{pmatrix} -cos2\theta & sin2\theta \\ sin2\theta & cos2\theta \end{pmatrix}]\begin{pmatrix} \nu_\alpha \\ \nu_\beta \end{pmatrix} \tag{47}$$

Now, let's suppose that the neutrinos are moving in a non-zero potential. Then you have to add a potential term to Schrodinger Equation

$$i\frac{d}{dt}\begin{pmatrix} \nu_\alpha \\ \nu_\beta \end{pmatrix} = (H_f + V)\begin{pmatrix} \nu_\alpha \\ \nu_\beta \end{pmatrix} \tag{48}$$

There is nothing to suggest that the interaction potential that ν_α experiences is the same as that which ν_β experiences. Hence, labelling the potential that ν_α experiences as V_α and the potential that ν_β experiences as V_β then

$$i\frac{d}{dt}\begin{pmatrix} \nu_\alpha \\ \nu_\beta \end{pmatrix} = [H_0 + \begin{pmatrix} -\frac{\Delta m^2}{4E}cos2\theta + V_\alpha & \frac{\Delta m^2}{4E}sin2\theta \\ \frac{\Delta m^2}{4E}sin2\theta & \frac{\Delta m^2}{4E}cos2\theta + V_\beta \end{pmatrix}]\begin{pmatrix} \nu_\alpha \\ \nu_\beta \end{pmatrix} \tag{49}$$

Now, we can always add a constant to this without affecting the final result, because that constant will eventually appear as a constant phase. When I take the modulus squared to get the probability, that constant phase will vanish. So, I'll add a term proportional to $-V_\beta$ so Equation 49 becomes

$$i\frac{d}{dt}\begin{pmatrix} \nu_\alpha \\ \nu_\beta \end{pmatrix} = [H_0 + \begin{pmatrix} -\frac{\Delta m^2}{4E}cos2\theta + (V_\alpha - V_\beta) & \frac{\Delta m^2}{4E}sin2\theta \\ \frac{\Delta m^2}{4E}sin2\theta & \frac{\Delta m^2}{4E}cos2\theta \end{pmatrix}]\begin{pmatrix} \nu_\alpha \\ \nu_\beta \end{pmatrix}^{2} \tag{50}$$

[2]This means that only differences in potential matter, not absolute potential. As usual.

What does this mean? Well, compare Equation 49 and Equation 47. The addition of the interaction potential difference means that we can no longer say that

$$\begin{pmatrix}\nu_\alpha\\ \nu_\beta\end{pmatrix} = \begin{pmatrix} cos\theta & sin\theta\\ -sin\theta & cos\theta\end{pmatrix}\begin{pmatrix}\nu_1\\ \nu_2\end{pmatrix} \tag{51}$$

The interaction has changed the mass eigenstates. You can get a picture of what is going on by thinking about throwing a cricket ball. In order to measure the mass of the ball, you can throw it with a given force and measure how far it goes. If the ball is thrown *with the same force* in a viscous liquid, which simulates the interaction of the neutrino with its environment through the potential, it will travel a shorter distance. If you couldn't see the liquid, you would imagine that it had a heavier mass than its rest mass in vacuum - interaction with the environment gives the ball a heavier *effective* mass. More rigorously, in a vacuum the neutrino mass eigenstate obeys the equation

$$E^2 - p^2 = m_i^2 \tag{52}$$

In a potential, V, this takes the form

$$(E+V)^2 - p^2 \approx m_i^2 + 2EV \tag{53}$$

. The effective mass of the neutrino is now $m_i' = \sqrt{m_i^2 + 2EV}$ So we need now to express Equation 50 in terms of mass eigenstates with mass eigenvalues equivalent to the effective masses, not the vacuum mass values.

What potential are we talking about and why is there a difference between ν_e and ν_μ? Taking the last part of that question first, we can see that there must be a difference in how the ν_e behaves in matter from how the ν_μ behaves in matter. Muon neutrinos produced in the solar core can *only* interact via the neutral current. They don't have enough energy to create a charged muon in the charged current process. Electron neutrinos, however, can interact via both the charged and neutral currents. The Feynman diagrams are shown in Figure 14. Hence the electron neutrinos can interact differently from the other types of neutrinos. Although it won't be important for our argument, the potential difference we are concerned about has the form

$$V_\alpha - V_\beta = 2\sqrt{2}G_F E N_e \tag{54}$$

where G_F is the Fermi constant, E is the neutrino energy and N_e is the electron number density in matter. This is sensible as (i) the cross section is a linear function of energy and (2) the more electrons there are, the more charged current interactions the ν_e can have and the larger the difference between ν_e and ν_μ.

Transforming the flavour Hamiltonian back into the vacuum mass basis using the mixing matrix, U, we get

$$\begin{aligned}
i\frac{d}{dt}\begin{pmatrix}\nu_1\\ \nu_2\end{pmatrix} &= U^\dagger i\frac{d}{dt}\begin{pmatrix}\nu_\alpha\\ \nu_\beta\end{pmatrix} && (55)\\
&= U^\dagger[H_0 + \begin{pmatrix} -\frac{\Delta m^2}{4E}cos2\theta + (V_\alpha - V_\beta) & \frac{\Delta m^2}{4E}sin2\theta\\ \frac{\Delta m^2}{4E}sin2\theta & \frac{\Delta m^2}{4E}cos2\theta\end{pmatrix}]\begin{pmatrix}\nu_\alpha\\ \nu_\beta\end{pmatrix} && (56)\\
&= (U^\dagger[H_0 + \begin{pmatrix} -\frac{\Delta m^2}{4E}cos2\theta & \frac{\Delta m^2}{4E}sin2\theta\\ \frac{\Delta m^2}{4E}sin2\theta & \frac{\Delta m^2}{4E}cos2\theta\end{pmatrix}]U + U^\dagger\begin{pmatrix} V_\alpha - V_\beta & 0\\ 0 & 0\end{pmatrix}U]\begin{pmatrix}\nu_1\\ \nu_2\end{pmatrix} && (57)\\
&= \frac{1}{2E}[\begin{pmatrix} m_1^2 & 0\\ 0 & m_2^2\end{pmatrix} + \begin{pmatrix} \Delta V cos^2\theta & \Delta V cos\theta sin\theta\\ \Delta V cos\theta sin\theta & \Delta V sin^2\theta\end{pmatrix}]\begin{pmatrix}\nu_1\\ \nu_2\end{pmatrix} && (58)\\
&= [\frac{1}{2E}\begin{pmatrix} m_1^2 + \Delta V cos^2\theta & \Delta V cos\theta sin\theta\\ \Delta V cos\theta sin\theta & m_2^2 + \Delta V sin^2\theta\end{pmatrix}]\begin{pmatrix}\nu_1\\ \nu_2\end{pmatrix} && (59)
\end{aligned}$$

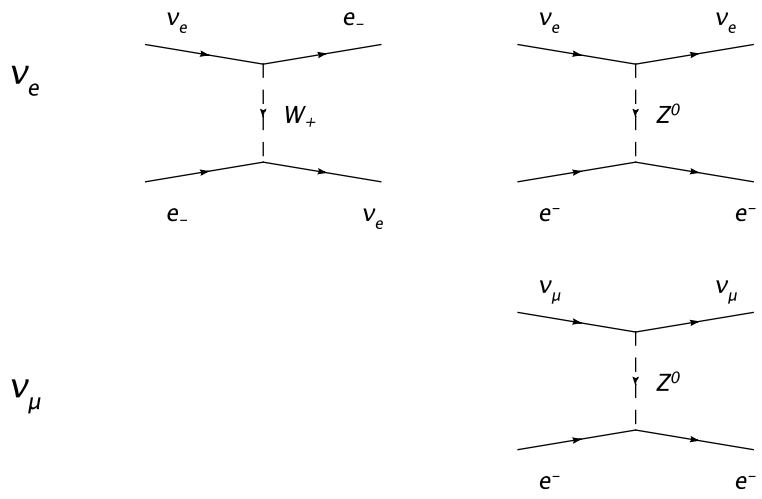

Figure 14: Interactions that the electron and muon neutrinos can have in the sun. Muon neutrinos can only interact via the neutral current, whereas electron neutrinos can interact via both the charged and neutral currents.

where I have defined $\Delta V \equiv V_\alpha - V_\beta$.

Notice that the mass matrix is no longer diagonal. This means that the mass eigenstates in the vacuum are not eigenstates of the Hamiltonian in matter. In order to get the correct eigenstates, we need to diagonalise this matrix. When we do this we find the modified mass eigenvalues in matter, m_{1m} and m_{2m} are

$$m^2_{1m,2m} = \frac{1}{2}[(m_1^2 + m_2^2 + \Delta V) \pm \sqrt{(\Delta V - \Delta m^2 cos2\theta)^2 + (\Delta m^2)^2 sin^2 2\theta} \tag{60}$$

with a mass splitting of

$$\Delta m^2_m = m^2_{1m} - m^2_{2m} = \Delta m^2 \sqrt{(\Delta V/\Delta m^2 - cos2\theta)^2 + sin^2 2\theta} \tag{61}$$

We can now perform the standard oscillation analysis to find a mixing angle θ_m which links the new mass eigenstates with the flavour states. To cut a long story short, we find that

$$sin2\theta_m = \frac{sin2\theta}{\sqrt{(\Delta V/\Delta m^2 - cos2\theta)^2 + sin^2 2\theta}} \tag{62}$$

The oscillation probabilities still have the same form as the standard two-flavour mixing, but are now expressed in terms of the mass eigenstates in matter and the matter modified mixing angle :

$$P_m(\nu_e \to \nu_\mu) = sin^2(2\theta_m) sin^2(1.27\Delta m^2_m \frac{L}{E}) \tag{63}$$

6.1.1 Observations

Let us consider the results for Δm^2_m and $sin^2 2\theta_m$ for a moment.

- If $\Delta V = 0$ (i.e. when in the vacuum where there is no matter to provide a potential difference), then $\Delta m^2_m = \Delta m^2$ and $sin^2 2\theta_m = sin^2 2\theta$. That is, in the vacuum the matter modified parameters reduce to the vacuum parameters. Good.

- If $sin^2 2\theta = 0$, then $sin^2 2\theta_m = 0$, regardless of the potential. For there to be oscillations in matter, one must already have the possibility of vacuum mixing.
- if the matter is very dense, $\Delta V \to \infty$, then $sin^2 2\theta_m \to 0$. In very dense matter, oscillations cannot occur via matter effects or otherwise.
- if $\Delta V/\Delta m^2 = cos 2\theta$ then the matter mixing angle is 1.0 - regardless of the value of the vacuum mixing angle. This is interesting. Even if the vacuum mixing is tiny, there may still be some value of the electron number density where the probability of oscillations is 100%. This is called the MSW resonance.
- Notice that if $\Delta m^2 \to -\Delta m^2$ in Equation 62, the term $(\Delta V/\Delta m^2 - cos 2\theta)$ in the denominator will have a different value and the effective mixing angle will be different. Using matter effects we can obtain an estimate for the *sign* of the mass difference. **Matter effects provide the only means by which we can determine the sign of the mass difference - it cannot be done with vacuum oscillations.**

So what is going on in the sun? Well, suppose the electron neutrino is born in the solar core in conditions of high density. According to our results, it cannot oscillate there. It starts to propagate outwards from the core, towards the vacuum. At some point, between the core and the vacuum, it crosses a region of the sun with electron number density that fulfills the resonance condition. In that region it oscillates from ν_e to ν_μ. Once out of this region, the matter density is too small to support matter oscillations, and the ν_μ leaves the sun to travel to earth.

In other words, some solar neutrinos *do not* oscillate on their way from the edge of the sun to earth. They have already oscillated by the time they get to the outer regions of the sun. They are generated as ν_e and leave the sun as ν_μ.

I say "some" because the situation is furthur complicated by energy dependence. Some neutrinos have so low an energy that they don't oscillate in the sun, but do in the vacuum. If one plugs the solar parameters (below) into the two-flavour oscillation formula, one finds that the survival probability $P(\nu_e \to \nu_e)$ is about 57%. This explains the different fractions of ν_e observed by experiments with different thresholds. At low energies, more neutrinos leave the sun without oscillating, but have a 50% change of oscillating on the journey from sun to earth. As the energy increases, the probability of oscillation within the sun through the matter effect increases, so the survival probability decreases. We believe, incidentally, that matter enhanced oscillation predominantly affects the ^7Be flux, but the p-p flux should be minimally affected. More experiments capable of probing the very low energy solar flux, in order to check this, are being built and run as I write (see the Borexino experiment, for example).

6.1.2 Solar Results

After analysis of all the solar data we find that it can be explained by the parameters

$$\Delta m^2_{sol} = (7.6 \pm 0.2) \times 10^{-5} \text{eV}^2 \qquad sin^2(2\theta_{sol}) = 0.8 \pm 0.1 \tag{64}$$

and that the oscillation is almost completely $\nu_e \to \nu_\mu$. It's interesting to note that the solar mixing angle is *not* maximal - $\theta \approx 32^\circ$.

6.2 Verification of the solar oscillation parameters

In order to check the solar oscillation analysis we need to make an experiment which is sensitive to $\Delta m^2 \approx 10^{-5}$ eV^2. We can't really do this with accelerators at the moment. The sort of energies one derives at accelerators is on the order of 1 GeV or larger, implying a baseline of $L > 100000$ km. That's about 10 times the diameter of the planet.

Instead we make use of the other artifical terrestrial neutrino source - reactors. These produce electron anti-neutrinos with energies around 5 MeV. Using these as a source, one only requires a baseline of about 100 km.

The experiment KamLAND is a liquid scintillator detector sited in the Kamioka mine next to Super-Kamiokande in Japan. Japan has a thriving nuclear power industry, and at least 50 nuclear power stations are close enough to Kamioka (see Figure 15) that KamLAND is capable of detecting $\overline{\nu_e}$ from them. Since the energy of the antineutrinos is very low, KamLAND has to be extremely pure, else it will be overloaded by background from the radioactive decay of other isotopes in the local region or in the detector itself.

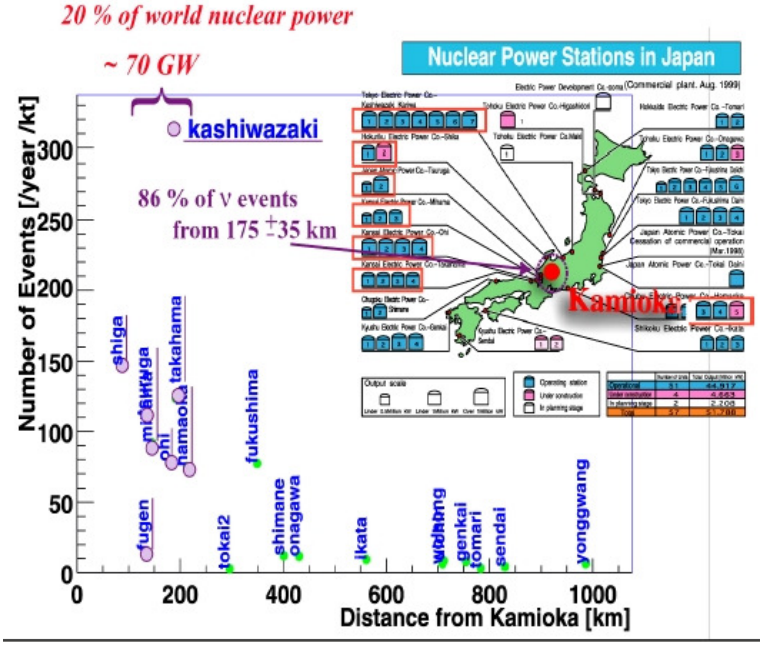

Figure 15: Locations of all nuclear reactors visible from the KamLAND detector.

KamLAND is a disappearance experiment. It has an advantage that the amount of matter between the detector and the reactors is too small to support any type of MSW effect, so KamLAND should measure the true solar vacuum oscillation parameters. Reactors produce pure beams of $\overline{\nu_e}$, so KamLAND trys to measure a deficit in the number of antineutrinos observed. Figure 16 shows the solar oscillation parameter allowed region in the $(sin^2\theta_{13}, \Delta m^2_{12})$ plane as measured by KamLAND and by a compilation of the solar neutrino experiments. The best fit points for the solar oscillation parameters are $(sin^2 2\theta_{12}, \Delta m^2_{12})_{best} = (0.304^{+0.022}_{-0.016}, 7.65^{+0.23}_{-0.20} \times 10^{-3}$ eV$^2)$. Notice, by the way, the complementarity between KamLAND and the other solar experiments. The experiments viewing the sun have large statistical power, but poor energy resolution, leading to the vertical elliptical error ellipse in the allowed region. KamLAND, on the other hand, doesn't see many events, but knows

what their energy is, so sets a more horizontal ellipse. The two constrain the allowed region to the small red region where both experiments are consistent.

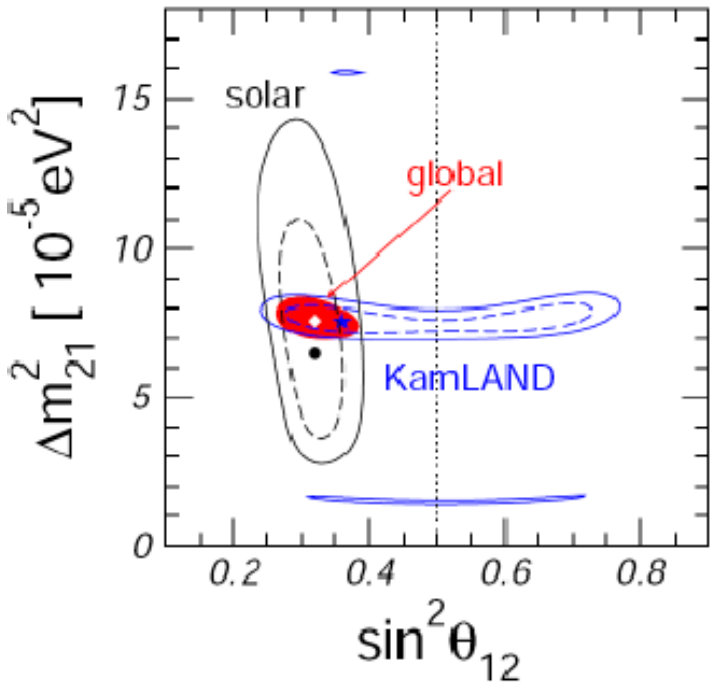

Figure 16: Allowed region for the solar oscillation parameters. Here the best fit values are $(sin^2 2\theta_{12}, \Delta m^2_{12})_{best} = (0.304^{+0.022}_{-0.016}, 7.65^{+0.23}_{-0.20} \times 10^{-3}$ eV$^2)$.

Figure 17 results shows a plot of the ratio of the observed to expected antineutrino events for an average L/E (an average since the neutrino sources are at different baselines - KamLAND just assigns all the events to an average L). This figure is the first actual proof that oscillations are happening - it's the first picture of an *oscillation*. KamLAND's analysis, combined with the other solar experiments, yielded

$$\Delta m^2_{sol} = 7.9 \times 10^{-5}\text{eV}^2 \qquad sin^2(2\theta_{sol}) = 0.81 \tag{65}$$

6.3 What you should know

- The general properties (both process and implications) of matter effects in neutrino oscillations (note : not the mathematics). One need only know that ν_e experiences interactions in matter than the other flavours do not. This modifies the mixing angle and the mass squared difference from their vacuum values.

- How neutrino oscillations explain the solar results, and how this was confirmed using the KamLAND detector.

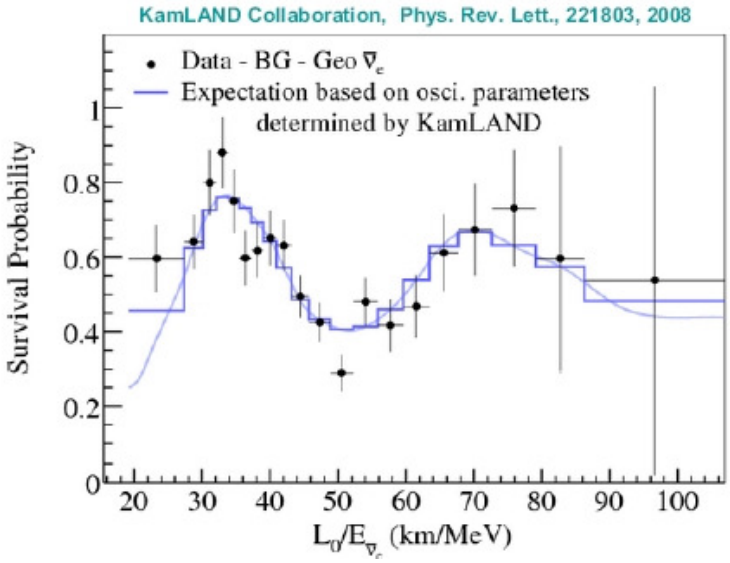

Figure 17: Ratio of observed to expected antineutrino rates as a function of the average L/E at KamLAND

7 Three Neutrino Oscillations

Of course, there are more than two neutrinos. There are three, and that implies that the mixing matrix can be (i) 3x3 , (ii) complex and (iii) unitary. In this case we have

$$\begin{pmatrix} \nu_e \\ \nu_\mu \\ \nu_\tau \end{pmatrix} = \begin{pmatrix} U_{e1} & U_{e2} & U_{e3} \\ U_{\mu 1} & U_{\mu 2} & U_{\mu 3} \\ U_{\tau 1} & U_{\tau 2} & U_{\tau 3} \end{pmatrix} \begin{pmatrix} \nu_1 \\ \nu_2 \\ \nu_3 \end{pmatrix} \tag{66}$$

This is known as the Pontecorvo-Maka-Nakagawa-Sakata (PMNS) matrix and does the same job in the neutrino sector as the CKM matrix does in the quark sector.

The fact that the matrix is unitary means that

$$U^\dagger U = I \quad \rightarrow \quad U^\dagger = U^{-1} = (U^*)^T \tag{67}$$

and from this

$$\begin{pmatrix} \nu_1 \\ \nu_2 \\ \nu_3 \end{pmatrix} = \begin{pmatrix} U^*_{e1} & U^*_{\mu 1} & U^*_{\tau 1} \\ U^*_{e2} & U^*_{\mu 2} & U^*_{\tau 2} \\ U^*_{e3} & U^*_{\mu 3} & U^*_{\tau 3} \end{pmatrix} \begin{pmatrix} \nu_e \\ \nu_\mu \\ \nu_\tau \end{pmatrix} \tag{68}$$

The unitarity of the PMNS matrix gives several useful relations:

$$\begin{pmatrix} U_{e1} & U_{e2} & U_{e3} \\ U_{\mu 1} & U_{\mu 2} & U_{\mu 3} \\ U_{\tau 1} & U_{\tau 2} & U_{\tau 3} \end{pmatrix} \begin{pmatrix} U^*_{e1} & U^*_{\mu 1} & U^*_{\tau 1} \\ U^*_{e2} & U^*_{\mu 2} & U^*_{\tau 2} \\ U^*_{e3} & U^*_{\mu 3} & U^*_{\tau 3} \end{pmatrix} = \begin{pmatrix} 1 & 0 & 0 \\ 0 & 1 & 0 \\ 0 & 0 & 1 \end{pmatrix} \tag{69}$$

so

$$\begin{aligned} U_{e1}U_{e1}^* + U_{\mu 1}U_{\mu 1}^* + U_{\tau 1}U_{\tau 1}^* &= 1 \\ U_{e2}U_{e2}^* + U_{\mu 2}U_{\mu 2}^* + U_{\tau 2}U_{\tau 2}^* &= 1 \\ U_{e3}U_{e3}^* + U_{\mu 3}U_{\mu 3}^* + U_{\tau 3}U_{\tau 3}^* &= 1 \\ U_{e1}U_{\mu 1}^* + U_{e2}U_{\mu 2}^* + U_{e3}U_{\mu 3}^* &= 0 \\ U_{e1}U_{\tau 1}^* + U_{e2}U_{\tau 2}^* + U_{e3}U_{\tau 3}^* &= 0 \\ U_{\mu 1}U_{\tau 1}^* + U_{\mu 2}U_{\tau 2}^* + U_{\mu 3}U_{\tau 3}^* &= 0 \end{aligned} \tag{70}$$

The oscillation probability is calculated just as before. Assume that at time t=0, we create a neutrino in a pure $|\nu_\alpha>$ state.

$$|\psi(x=0)>= U_{\alpha 1}|\nu_1> + U_{\alpha 2}|\nu_2> + U_{\alpha 3}|\nu_3> \tag{71}$$

The wavefunction evolves as

$$|\psi(t)>= U_{\alpha 1}|\nu_1> e^{-ip_1\cdot x} + U_{\alpha 2}|\nu_2> e^{-ip_2\cdot x} + U_{\alpha 3}|\nu_3> e^{-ip_3\cdot x} \tag{72}$$

where $p_i \cdot x = E_i t - \mathbf{p_i}\cdot\mathbf{x}$. After travelling a distance L the wavefunction is (assuming that the neutrino is relativistic)

$$|\psi(L)>= U_{\alpha 1}|\nu_1> e^{-i\phi_1} + U_{\alpha 2}|\nu_2> e^{-i\phi_2} + U_{\alpha 3}|\nu_3> e^{-i\phi_3} \tag{73}$$

with $\phi_i = p_i\cdot x = E_i t - |p_i|L \approx (E_i - |p_i|)L$. As before, we can approximate E_i by

$$E_i \approx p_i + \frac{m_i^2}{2E_i} \tag{74}$$

so

$$\phi_i = (E_i - |p_i|)L \approx \frac{m_i^2}{2E_i}L \tag{75}$$

.

Expressing the mass eigenstates in terms of the flavour eigenstates:

$$\begin{aligned} |\psi(L)>=& U_{\alpha 1}e^{-i\phi_1}(U_{e1}^*|\nu_e> + U_{\mu 1}^*|\nu_\mu> + U_{\tau 1}^*|\nu_\tau>) \\ &+ U_{\alpha 2}e^{-i\phi_2}(U_{e2}^*|\nu_e> + U_{\mu 2}^*|\nu_\mu> + U_{\tau 2}^*|\nu_\tau>) \\ &+ U_{\alpha 3}e^{-i\phi_3}(U_{e3}^*|\nu_e> + U_{\mu 3}^*|\nu_\mu> + U_{\tau 3}^*|\nu_\tau>) \end{aligned} \tag{76}$$

which can be arranged to give

$$\begin{aligned} |\psi(L)>=& (U_{\alpha 1}U_{e1}^*e^{-i\phi_1} + U_{\alpha 2}U_{e2}^*e^{-i\phi_2} + U_{\alpha 3}U_{e3}^*e^{-i\phi_3})|\nu_e> \\ &+ (U_{\alpha 1}U_{\mu 1}^*e^{-i\phi_1} + U_{\alpha 2}U_{\mu 2}^*e^{-i\phi_2} + U_{\alpha 3}U_{\mu 3}^*e^{-i\phi_3})|\nu_\mu> \\ &+ (U_{\alpha 1}U_{\tau 1}^*e^{-i\phi_1} + U_{\alpha 2}U_{\tau 2}^*e^{-i\phi_2} + U_{\alpha 3}U_{\tau 3}^*e^{-i\phi_3})|\nu_\tau> \end{aligned} \tag{77}$$

from which we can get the oscillation probability $P(\nu_\alpha \to \nu_\beta)$:

$$\begin{aligned} P(\nu_\alpha \to \nu_\beta) =& |<\nu_\beta|\psi(L)>|^2 \\ =& (U_{\alpha 1}U_{\beta 1}^*e^{-i\phi_1} + U_{\alpha 2}U_{\beta 2}^*e^{-i\phi_2} + U_{\alpha 3}U_{\beta 3}^*e^{-i\phi_3})^2 \end{aligned} \tag{78}$$

Using the complex relationship

$$|z_1 + z_2 + z_3|^2 = |z_1|^2 + |z_2|^2 + |z_3|^2 + 2\Re(z_1 z_2^* + z_1 z_3^* + z_2 z_3^*) \tag{79}$$

we can write Equation 78 as (eventually - I will never ask you to do this derivation))

$$\begin{aligned} P(\nu_\alpha \to \nu_\beta) =& \delta_{\alpha\beta} - 4\sum_{i>j} Re(U^*_{\alpha i} U_{\beta i} U_{\alpha j} U^*_{\beta j}) sin^2(\Delta m^2_{ij} \frac{L}{4E}) \\ &+ 2\sum_{i>j} Im(U^*_{\alpha i} U_{\beta i} U_{\alpha j} U^*_{\beta j}) sin(\Delta m^2_{ij} \frac{L}{2E}) \end{aligned} \tag{80}$$

The PMNS matrix is usually expressed by 3 rotation matrices and three complex phases:

$$U = \begin{pmatrix} 1 & 0 & 0 \\ 0 & cos\theta_{23} & sin\theta_{23} \\ 0 & -sin\theta_{23} & cos\theta_{23} \end{pmatrix} \begin{pmatrix} cos\theta_{13} & 0 & sin\theta_{13} e^{-i\delta_{CP}} \\ 0 & 1 & 0 \\ -sin\theta_{13} e^{i\delta_{CP}} & 0 & cos\theta_{13} \end{pmatrix} \begin{pmatrix} cos\theta_{12} & sin\theta_{12} & 0 \\ -sin\theta_{12} & cos\theta_{12} & 0 \\ 0 & 0 & 1 \end{pmatrix} \begin{pmatrix} 1 & 0 & 0 \\ 0 & e^{i\beta} & 0 \\ 0 & 0 & e^{i\gamma} \end{pmatrix} \tag{81}$$

The final sub-matrix in this expression include the so-called *Majorana phases*, $e^{i\beta}$ and $e^{i\gamma}$. This matrix plays no part in the description of neutrino flavour oscillations so we will ignore it for now. It does, however, play a part in neutrinoless double beta decay.

Ignoring the Majorana phases, we find that, when multplied out, the PMNS matrix is

$$U = \begin{pmatrix} c_{12}c_{13} & s_{12}c_{13} & s_{13}e^{-i\delta_{CP}} \\ -s_{12}c_{23} - c_{12}s_{23}s_{13}e^{i\delta_{CP}} & c_{12}c_{23} - s_{12}s_{13}s_{23}e^{i\delta_{CP}} & c_{13}s_{23} \\ s_{12}s_{23} - c_{12}s_{13}c_{23}e^{i\delta_{CP}} & -c_{12}s_{23} - s_{12}s_{13}c_{23}e^{i\delta_{CP}} & c_{13}c_{23} \end{pmatrix} \tag{82}$$

where $c_{ij} = cos\theta_{ij}$ and $s_{ij} = sin\theta_{ij}$. The first matrix is called the "12-sector", the second matrix is the "13-sector", and the third is the "23-sector". The second matrix is responsible, possibly, for CP-violation. We'll talk about that below. For now let's set δ_{CP} to zero. If this is the case, then the imaginary term in Equation 80 vanishes and we are left with

$$P(\nu_\alpha \to \nu_\beta) \quad = \quad \delta_{\alpha\beta} - 4\sum_{i>j} (U_{\alpha i} U_{\beta i} U_{\alpha j} U_{\beta j}) sin^2(\Delta m^2_{ij} \frac{L}{4E}) \tag{83}$$

We also must remember the squared mass difference. There are 3 neutrino mass eigenstates, and hence 2 independent mass splittings, called Δm^2_{23} and Δm^2_{12}. The other splitting is defined by the relationship

$$\Delta m^2_{12} + \Delta m^2_{23} + \Delta m^2_{31} = 0 \tag{84}$$

We know from the solar and atmospheric neutrino problems that these splittings have values around $+8 \times 10^{-5}$ eV^2 and 3×10^{-3} eV^2. To go ahead a bit, the mass splitting relating to the 23 sector is the atmospheric neutrino mass difference : $\Delta m^2_{23} = 3 \times 10^{-3}$eV^2 and the splitting relating to the 12 sector is the solar mass difference : $\Delta m^2_{12} = 8 \times 10^{-5}$eV^2

Let's consider an appearance experiment. In this case $\alpha \neq \beta$. Then

$$\begin{aligned} P(\nu_\alpha \to \nu_\beta) = & -4\sum_{i>j}(U_{\alpha i}U_{\beta i}U_{\alpha j}U_{\beta j})sin^2(1.27\Delta m^2_{ij}\frac{L}{E}) \\ = & -4[(U_{\alpha 1}U_{\beta 1}U_{\alpha 2}U_{\alpha 2})sin^2(1.27\Delta m^2_{12}\frac{L}{E}) \\ & + (U_{\alpha 1}U_{\beta 1}U_{\alpha 3}U_{\alpha 3})sin^2(1.27\Delta m^2_{13}\frac{L}{E}) \\ & + (U_{\alpha 2}U_{\beta 2}U_{\alpha 3}U_{\alpha 3})sin^2(1.27\Delta m^2_{23}\frac{L}{E})] \end{aligned} \tag{85}$$

Equation 85 can be split into two cases. The first occurs for experiments where L/E is small. In this case, $\Delta m^2_{12}L/E$ is very small and

$$sin^2(1.27\Delta m^2_{12}\frac{L}{E}) \to 0 \tag{86}$$

So, with the reasonable approximation that $\Delta m^2_{13} \approx \Delta m^2_{23}$,

$$P(\nu_\alpha \to \nu_\beta) = -4[U_{\alpha 1}U_{\beta 1}U_{\alpha 3}U_{\beta 3} + U_{\alpha 2}U_{\beta 2}U_{\alpha 3}U_{\beta 3}]sin^2(1.27\Delta m^2_{23}\frac{L}{E}) \tag{87}$$

The other case occurs when L/E is large. Then the terms involving Δm^2_{23} and Δm^2_{13} are rapidly oscillating and average to 0.5

$$sin^2(1.27\Delta m^2_{23}\frac{L}{E}) \to < sin^2(1.27\Delta m^2_{23}\frac{L}{E}) >= \frac{1}{2} \tag{88}$$

$$sin^2(1.27\Delta m^2_{13}\frac{L}{E}) \to < sin^2(1.27\Delta m^2_{13}\frac{L}{E}) >= \frac{1}{2} \tag{89}$$

and

$$\begin{aligned} P(\nu_\alpha \to \nu_\beta) = & -4[(U_{\alpha 1}U_{\beta 1}U_{\alpha 2}U_{\beta 2})sin^2(1.27\Delta m^2_{12}\frac{L}{E}) \\ & + \frac{1}{2}(U_{\alpha 1}U_{\beta 1}U_{\alpha 3}U_{\beta 3} + U_{\alpha 2}U_{\beta 2}U_{\alpha 3}U_{\beta 3})] \end{aligned} \tag{90}$$

Replacing the elements U_{ij} with the mixing angle terms from the PMNS matrix, and remembering that $\delta_{CP} = 0$, we can use the unitarity relations in Equation set 70 to get (after a while) for the small L/E case

$$P(\nu_\mu \to \nu_\tau) = \cos^4(\theta_{13})\sin^2(2\theta_{23})\sin^2(1.27\Delta m^2_{23}\frac{L}{E}) \tag{91}$$

$$P(\nu_e \to \nu_\mu) = \sin^2(2\theta_{13})\sin^2(\theta_{23})\sin^2(1.27\Delta m^2_{23}\frac{L}{E}) \tag{92}$$

$$P(\nu_e \to \nu_\tau) = \sin^2(2\theta_{13})\cos^2(\theta_{23})\sin^2(1.27\Delta m^2_{23}\frac{L}{E}) \tag{93}$$

and for the large L/E case

$$P(\nu_e \to \nu_{\mu,\tau}) = \cos^2(\theta_{13})\sin^2(2\theta_{12})\ \sin^2(1.27\Delta m^2_{12}\frac{L}{E}) + \frac{1}{2}\sin^2(2\theta_{13}) \tag{94}$$

Now, if $\theta_{13} = 0$ then these equations reduce to:

- Small L/E :

$$\begin{aligned} P(\nu_\mu \to \nu_\tau) &= \sin^2(2\theta_{23})\sin^2(1.27\Delta m^2_{23}\frac{L}{E}) \\ P(\nu_e \to \nu_\mu) &= 0 \\ P(\nu_e \to \nu_\tau) &= 0 \end{aligned}$$

- Large L/E :

$$P(\nu_e \to \nu_{\mu,\tau}) = \sin^2(2\theta_{12})\,\sin^2(1.27\Delta m^2_{12}\frac{L}{E}) \tag{95}$$

These are the same equations we used for the atmospheric and solar oscillations. We therefore identify the 23-sector with atmospheric neutrinos with a $\Delta m^2_{23} \approx 3 \times 10^{-3}$ eV^2, and the 12-sector with solar neutrinos with a $\Delta m^2_{12} \approx 8 \times 10^{-5}$ eV^2.

We have some information about the atmospheric and solar oscillation sectors. We also know that $P(\nu_\mu \to \nu_e)$ is small for atmospheric neutrinos. This suggests that θ_{13} is small too. Can we do better?

7.1 How to measure θ_{13}

We would like to be able to determine θ_{13} without having to include the other mixing angles. This is because, although measured, they have large errors, and inclusion will just make the θ_{13} measurement more imprecise. We can do this by looking at the survival probability $P(\nu_e \to \nu_e)$. Going back to Equation 85, we can write

$$\begin{aligned} P(\nu_e \to \nu_e) = 1 - 4[&U^2_{e1}U^2_{e2}sin^2(1.27\Delta m^2_{12}\frac{L}{E}) \\ &+ U^2_{e1}U^2_{e3}sin^2(1.27\Delta m^2_{13}\frac{L}{E}) \\ &+ U^2_{e2}U^2_{e3}sin^2(1.27\Delta m^2_{23}\frac{L}{E})] \end{aligned} \tag{96}$$

Since $\Delta m^2_{13} \approx \Delta m^2_{23}$ and, from the unitarity conditions, $U^2_{e1} + U^2_{e2} + U^2_{e3} = 1$

$$\begin{aligned} P(\nu_e \to \nu_e) &= 1 - 4[U^2_{e1}U^2_{e2}sin^2(1.27\Delta m^2_{12}\frac{L}{E}) + U^2_{e3}(1 - U^2_{e3})sin^2(1.27\Delta m^2_{23}\frac{L}{E})] \\ &= 1 - 4[(cos\theta_{12}cos\theta_{13})^2(sin\theta_{12}cos\theta_{13})^2sin^2(1.27\Delta m^2_{12}\frac{L}{E}) \\ &+ sin^2(\theta_{13})(1 - sin^2(\theta_{13}))sin^2(1.27\Delta m^2_{23}\frac{L}{E})] \\ &= 1 - cos^4(\theta_{13})(2sin\theta_{12}cos\theta_{12})^2sin^2(1.27\Delta m^2_{12}\frac{L}{E}) \\ &- (2cos\theta_{13}sin\theta_{13})^2sin^2(1.27\Delta m^2_{23}\frac{L}{E}) \\ &= 1 - cos^4\theta_{13}sin^2(2\theta_{12})sin^2(1.27\Delta m^2_{12}\frac{L}{E}) - sin^2(2\theta_{13})sin^2(1.27\Delta m^2_{23}\frac{L}{E}) \end{aligned} \tag{97}$$

The first term has a contribution from the solar oscillation wavelength associated with the small mass splitting, Δm^2_{12},

$$\lambda_{sol} = 2.47\frac{E}{\Delta m^2_{12}}, \tag{98}$$

and the second term provides a contribution from the atmospheric oscillation wavelength associated with Δm^2_{23},

$$\lambda_{atm} = 2.47 \frac{E}{\Delta m^2_{23}}. \tag{99}$$

For a 1 MeV neutrino, $\lambda_{sol} = 33.0\ km$ with $\Delta m^2_{12} = 7.5 \times 10^{-5}$ eV^2, and $\lambda_{atm} = 1.0\ km$ with $\Delta m^2_{23} = 2.4 \times 10^{-3}$ eV^2. At MeV energies, the solar-scale oscillations are far slower than the atmospheric-scale oscillations as shown in Figure 18 in which you can see the fast atmospheric-scale oscillations superimposed on the slower solar-scale oscillations[3]

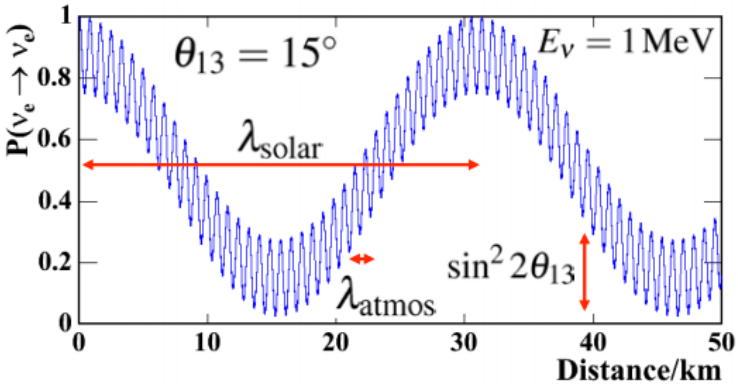

Figure 18: The ν_e survival probability with $\theta_{13} = 15°$, $\Delta m^2_{12} = 7.5 \times 10^{-5}$ eV^2, $\Delta m^2_{23} = 2.4 \times 10^{-3}$ eV^2 and $\theta_{12} = 33°$. The fast oscillations, governed by the atmospheric mass scale, is superimposed on the much slower solar-scale oscillation.

Close to the source, on a baseline of about a kilometre, we should only be sensitive to the atmospheric-scale oscillation term. The survival probability in this region is

$$P(\nu_e \to \nu_e) \approx 1 - sin^2(2\theta_{13}) sin^2(1.27 \Delta m^2_{23} \frac{L}{E}) \tag{100}$$

which eliminates all the other mixing angles. So all we need to do is find a ν_e beam with energy around a few MeV and put a detector at the right place, but on the scale of a kilometer of so from the source.

This is a bit difficult, however, as there are no known terrestrial ν_e sources which obey these conditions. One has two possibilities : look for ν_e appearing in an a ν_μ beam or try to use the $\overline{\nu_e}$ generated in vast quantities in nuclear reactors. In order to use the latter source we must first find a way to relate $P(\nu_e \to \nu_e)$ with $P(\overline{\nu_e} \to \overline{\nu_e})$?

7.1.1 C,P and T violation

Recall that there are three discrete symmetries used in particle physics:

- **Charge conjugation $\hat{C}$:** C changes particles to antiparticles

[3]Just to be clear - the solar oscillation is *not* the average of the pattern shown in Figure 18. The probability function is the sum of two different terms. The solar probability can be viewed as a line linking the top of the peaks in the oscillation pattern (so that the survival probability is 1.0 at zero distance). The atmospheric-scale oscillations subtracts a bit of survival probability from that baseline.

- **Parity $\hat{P}$:** P reverses the spatial components of wavefunctions
- **Time $\hat{T}$:** T reverses the interaction by running time backwards

The weak interaction violates $\hat{P}$. It also violates $\hat{C}$. Consider the decay in Figure 19. The decay is

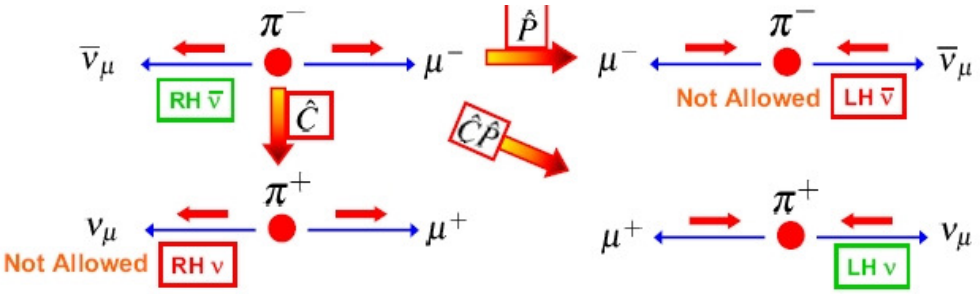

Figure 19: $\hat{C}$ and $\hat{P}$ violation in pion weak decay. The blue arrows are the particle, and the red arrows show the spin vectors of each particle.

$\pi^- \to \mu^- + \overline{\nu_\mu}$. Parity flips the direction of the particles, but not the spin, resulting in a left-handed antineutrino, which is not allowed. Charge conjugation changes particles to antiparticles, resulting in the decay $\pi^+ \to \mu^+ + \nu_\mu$, which would be fine, except that the neutrino is right-handed. This, again, is not allowed. However, the application of $\hat{C}\hat{P}$ changes left-handed particles into right-handed anti-particles and the resulting decay can happen. $\hat{C}\hat{P}$ invariance implies that the probability of a particular interaction happening is identical to the probability of the $\hat{C}\hat{P}$ transformed interaction occurring. Actually we know that $\hat{C}\hat{P}$ is violated at a low level in weak decay. We believe that $\hat{C}\hat{P}\hat{T}$ *has* to apply.

How do these symmetries affect neutrino oscillations?

- Time Reversal : This flips the time direction of the oscillation:

$$(\nu_\alpha \to \nu_\beta) \to (\nu_\beta \to \nu_\alpha) \tag{101}$$

. Invariance under time reversal implies that

$$P(\nu_\alpha \to \nu_\beta) = P(\nu_\beta \to \nu_\alpha) \tag{102}$$

- CP : This changes neutrinos to antineurtrinos and reverses all the spatial directions

$$(\nu_\alpha \to \nu_\beta) \to (\overline{\nu_\alpha} \to \overline{\nu_\beta}) \tag{103}$$

. Invariance under CP implies that

$$P(\nu_\alpha \to \nu_\beta) = P(\overline{\nu_\alpha} \to \overline{\nu_\beta}) \tag{104}$$

- CPT : This changes neutrinos to antineurtrinos, reverses all the spatial directions and changes the direction of time

$$(\nu_\alpha \to \nu_\beta) \to (\overline{\nu_\beta} \to \overline{\nu_\alpha}) \tag{105}$$

Invariance under CPT implies that

$$P(\nu_\alpha \to \nu_\beta) = P(\overline{\nu_\beta} \to \overline{\nu_\alpha}) \tag{106}$$

From the point of view of the ν_e experiment we were talking about above, CPT invariance implies that $P(\nu_e \to \nu_e) = P(\overline{\nu_e} \to \overline{\nu_e})$. Hence, the survival probability should be the same for electron antineutrinos from reactors as for electron neutrinos of the same energies :

$$P(\nu_e \to \nu_e) = 1 - sin^2(2\theta_{13})sin^2(1.27\Delta m^2_{23}\frac{L}{E}) = P(\overline{\nu_e} \to \overline{\nu_e}) \tag{107}$$

7.2 The measurement of θ_{13}

A good way, then, of measuring θ_{13} is to look at the disappearance of $\overline{\nu_e}$ in a flux of neutrinos from a reactor. The detector should be placed about 1 km away so there is no interference from the solar oscillation term. This was finally done in 2012 by three reactor experiments : Daya Bay in China, Double CHOOZ in France and RENO in South Korea. Of interest to this story is Daya Bay - a reactor experiment with the largest reach in measuring θ_{13}. Daya Bay is in Southern China, near Hong Kong. It comprises 6 nuclear reactor cores, providing a hugh flux of electron anti-neutrinos. The cores are viewed by six 20 ton liquid scintillator detectors at baselines of 360 m, 500 m and 1700 m from the reactors as shown in Figure 20 The addition of these medium baseline detectors are valuable in measuring the L/E behaviour of any oscillation observed.

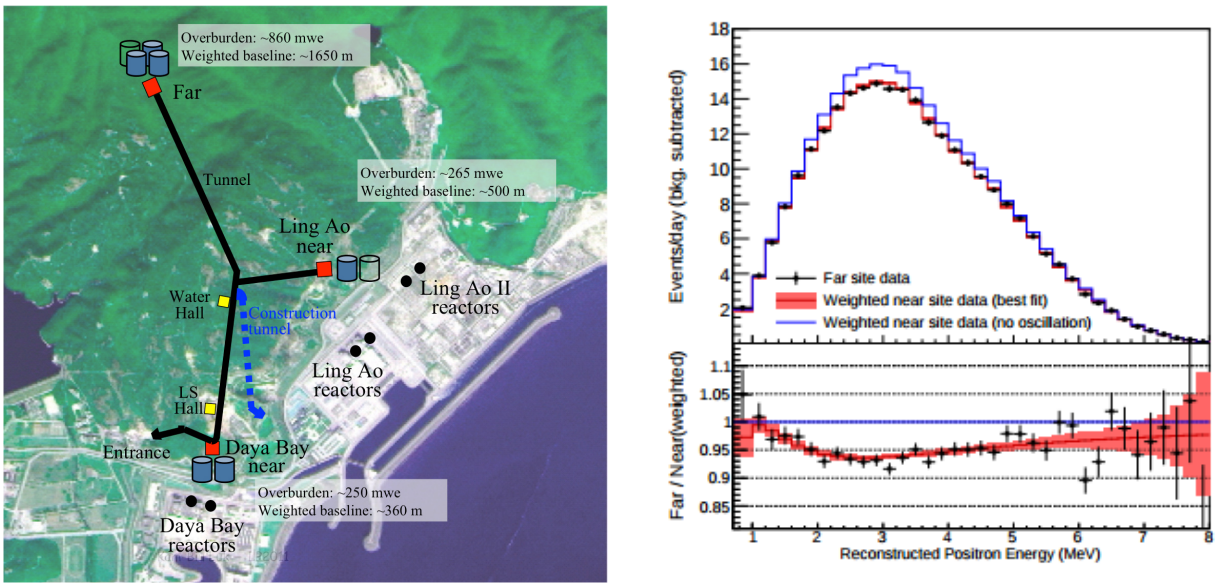

Figure 20: (left) A schematic of the Daya Bay experiment, showing the six reactor cores used to generate the $\overline{\nu_e}$ flux and the location of the 6 detectors at different baselines (right) Daya Bay's reported results. The histogram shows the energy spectrum of $\overline{\nu_e}$ expected in the absence of oscillations (blue histogram) and the measured energy spectrum (black dots).

In 2012 Daya Bay reported a positive measurement of $sin^2(2\theta_{13})$. This is shown on the right of Figure 20. The histogram shows the measured energy spectrum of $\overline{\nu_e}$ from the reactors in the absence of oscillations. The data points show the measurements. There is a clear deficit in the observed data at the peak. Futhermore, the deficit is baseline-dependent. If interpreted as arising from neutrino oscillations, this deficit can be used to measure θ_{13}. The result is $sin^2(2\theta_{13}) = 0.085 \pm 0.006$. This gives a mixing angle of $\theta_{13} \approx 8.6°$. This result was quickly validated by measurements from RENO

and Double CHOOZ who reported mixing angle measurements of $sin^2(2\theta_{13}) = 0.113 \pm 0.02$ and $sin^2(2\theta_{13}) = 0.107 \pm 0.05$. It seems that θ_{13} is actually quite large.

7.2.1 T2K Returns

T2K was mentioned above in the context of the measurement of Δm^2_{23} and $sin^2(2\theta_{23})$ using ν_μ disappearance. However, it was designed and built primarily to measure θ_{13} by looking for ν_e appearance in a ν_μ beam. The oscillation probability has been calculated above and is, in the two-flavour approximation,

$$P(\nu_\mu \rightarrow \nu_e) = sin^2(2\theta_{13})sin^2(\theta_{23})sin^2(1.27\Delta m^2_{23}\frac{L}{E}) \tag{108}$$

The T2K beam is almost pure ν_μ so the idea is to look for the appearance of electron-type neutrinos in the far detector, Super-Kamiokande. T2K uses the electron identification properties of the Super-Kamiokande detector.

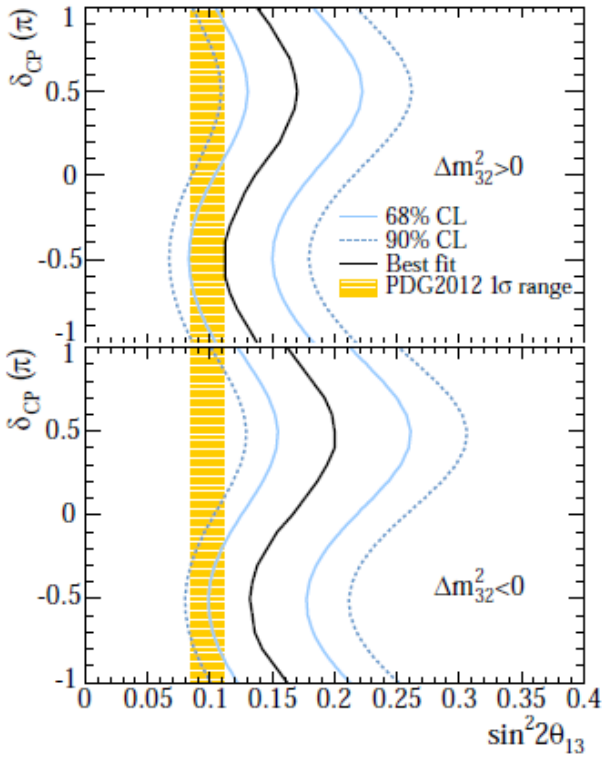

Figure 21: The 68as a function of δ_{CP} assuming normal hierarchy (top) and inverted hierarchy (bottom). The solid line represents the best fit $sin^2(2\theta_{13})$ value for the given δ_{CP} values. The shaded region shows the average θ_{13} from reactor experiments world-wide.

T2K switched on in mid-2010. In March 2011 it was hit by the Japanese earthquake and only started to taking data again a year later, in March 2012. It took neutrino-mode data until 2015, at which point it swapped the polarity of the beam and is now taking antineutrino data. In the electron neutrino apeearance search, the far detector recorded 28 electron neutrino interactions associated with the T2K beam. It expected to see 11 events from known background sources. The discrepancy represents a 7 σ positive result. The 68% and 90% confidence region for $sin^2(2\theta_{13})$ as a function of δ_{CP}

are shown in Figure 21. Normal hierarchy is shown on the top plot and inverted hierarchy is shown on the bottom plot. The shaded region shows the average θ_{13} result from the reactor experiments. Both the reactor experiments and T2K are consistent. One could argue that T2K data favours a $\delta_{CP} < 0$ (although not with any great statistical justification).

The global average of all θ_{13} results is

$$sin^2(2\theta_{13}) = 0.094^{+0.007}_{-0.009} \tag{109}$$

7.3 What you need to know

- How, and under what conditions, the three flavour neutrino oscillation probability splits into the "atmospheric" and the "solar" sectors.
- The importance of θ_{13} and the methods used to measure it. You don't need to know great detail - just the oscillations modes that are used to make the measurement and the result.

8 Summary of Current Knowledge and open questions

We can now summarise our current level of knowledge of neutrino oscillations and neutrino mass from oscillation experiments.

We now know that there are 3 light neutrinos. The neutrino mass states are different from the flavour states. There are two mass splittings

$$\Delta m^2_{12} = +7.54 \times 10^{-5}\text{eV}^2 \tag{110}$$

and

$$|\Delta m^2_{23}| = 2.4 \times 10^{-3}\text{eV}^2 \tag{111}$$

We know the sign of Δm^2_{12} but not Δm^2_{23}. This is shown in Figure 22. The mixing angles have now

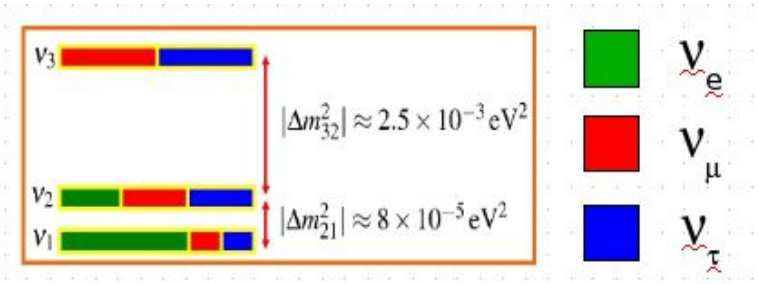

Figure 22: Current knowledge of neutrino mass eigenstate splitting (assuming θ_{13} is zero).

all been determined, to various levels of precision, and are shown in Table 2

8.1 Open Questions

There are a number of questions currently left open:

- We need to obtain better estimates of $sin^2(2\theta_{23}), \Delta m^2_{23}, sin^2(2\theta_{12})$ and Δm^2_{12}.

- Is $\theta_{23} = 45$ degrees or not?
- Is the mass hierarchy normal ($\Delta m^2_{23} > 0$) or inverted ($\Delta m^2_{23} < 0$)?
- Are the neutrinos and antineutrinos identical? This cannot be answered by an oscillation experiment.
- What is the absolute neutrino mass? This cannot be measured by an oscillation experiments.
- Why is the MNSP matrix so different in form to the CKM matrix? This will require a deeper understanding of flavour and mass generation mechanisms.
- What is the value of δ_{CP}?

The final question is the ultimate measurement we wish to make in neutrino physics and informs the future 20-25 years of the field.

8.2 What you should know

- The identify of each sub–matrix of the PMNS matrix. What do each of the correspond to, in terms of oscillations and what are the measured values of each of the mixing angles.
- The general state of parameter measurements (I won't expect detailed numbers but you should know the values of the mixing angles to the degree or so).
- What are the current open questions in neutrino physics?

9 A Spanner In The Works?

To date we have built up a nice coherent theory of 3-flavour neutrino oscillations that seems to be supported by the available data. I am now going to throw a handful of spanners into the machinery. These may be very heavy-duty spanners, which have the potential to stomp this nice framework into kindling (to recklessly mix my metaphors), or they may be light-weight chocolate spanners which won't survive being exposed to the sunlight of extra data (metaphor. mix.) - we don't know yet. The first spanner is called LSND.

9.1 LSND

The LSND detector (**L**iquid **S**cintillator **N**eutrino **D**etector) was the first oscillation experiment to report a positive result. It was an experiment designed to search for $\nu_\mu \to \nu_e$ oscillations through the appearance of a ν_e in the single near detector.

Parameter	Measurement	Angle
$sin^2(2\theta_{23})$	> 0.92	$(45.0 \pm 2.4)^\circ$
$sin^2(2\theta_{12})$	0.85 ± 0.03	$(33.6 \pm 0.8)^\circ$
$sin^2(2\theta_{13})$	0.084 ± 0.01	$(8.9 \pm 0.3)^\circ$

Table 2: Current results of measurements of all mixing angles in the PMNS matrix.

The beam used the Los Alamos Meson Physics Facility (LAMPF). LAMPF produced π^+ in a water target which came to rest within the target itself. The pions then decayed to produce $\overline{\nu_\mu}$ via the decay chain

$$\begin{aligned} \pi^+ &\rightarrow \mu^+ + \nu_\mu \\ \mu^+ &\rightarrow e^+ + \nu_e + \overline{\nu_\mu} \end{aligned}$$

The maximum energy of the ν_μ produced by this chain was 52.8 MeV and the experiment looked for $\overline{\nu_e}$ appearance in the $\overline{\nu_\mu}$ beam. The detector was located $30m$ from the neutrino source, making it sensitive to a $\Delta m^2 \approx 1.0$ eV^2.

The LSND detector was a tank filled with 167 tonnes of mineral oil doped with a scintillating compound. The mineral oil acted as a Cerenkov-emitter, so the internal volume of the tank was viewed by an array of 1220 photomultipler tubes. The scintillator emitted light isotropically but was used to tag the existance of charged particles below the Cerenkov threshold. The experiment looked for $\overline{\nu_e}$ interactions using inverse beta decay : $\overline{\nu_e} + p \rightarrow e^+ + n$ with the final state neutron being captured by the mineral oil to generate a 2.2 MeV photon. This coincidence between the prompt e^+ signal and the delayed photon signal distinguished such events form other backgrounds.

In 1996, LSND reported the observation of an excess of $\overline{\nu_e}$ above that expected in the absence of neutrino oscillations. The first data, shown in Figure 23, measured 22 events with 4.6±0.6 background events. If this excess is interpreted as $\overline{\nu_\mu}$ oscillation to $\overline{\nu_e}$, then the best fit oscillation points is at $(sin^2(2\theta), \Delta m^2_{23}) = (0.003, 1.2\text{eV}^2)$ with an allowed region as shown in Figure 23

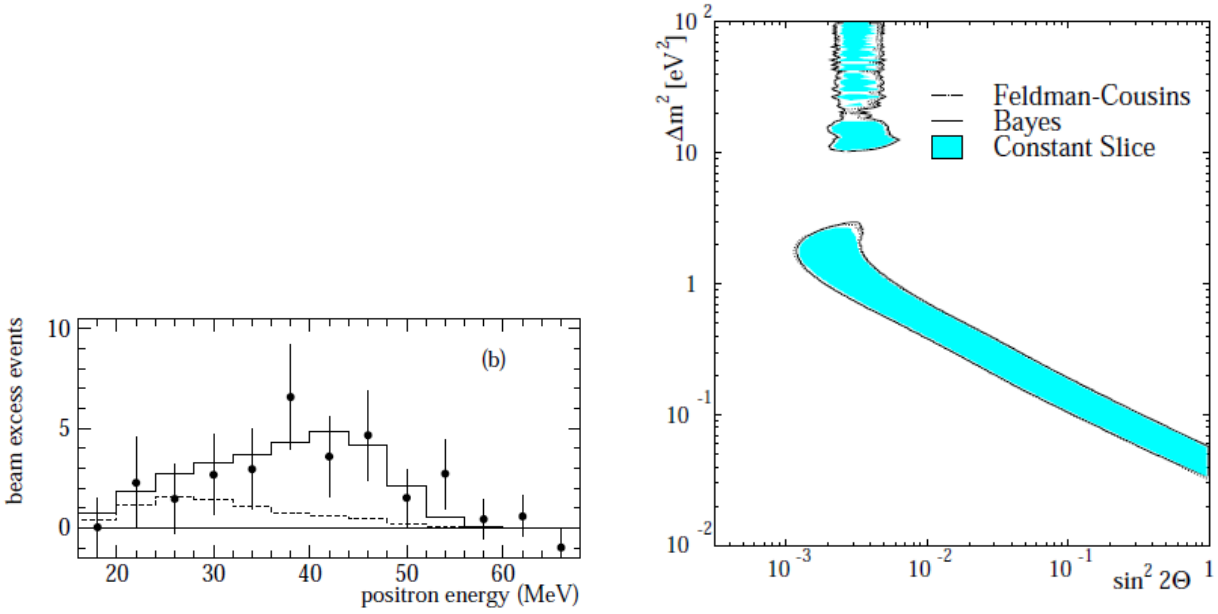

Figure 23: (Left) Excess of $\overline{\nu_e}$ observed in the LSND experiment. The dashed line is the expected background. The solid line shows what is expected including neutrino oscillations. The dots are the data. (Right) Allowed region from the LSND appearance analysis.

Although quite exciting at the time, the LSND result has become something of a pain. The reason is the value of Δm^2 that LSND found. We know from the solar and atmospheric experiments that there are are mass scales : $\Delta m^2_{12} = 8 \times 10^{-5}\text{eV}^2$ and $|\Delta m^2_{23}| = 2.3 \times 10^{-3}\text{eV}^2$. We also know that,

given N active neutrinos with a mass below half the Z^0 boson mass, there must be $N-1$ independent mass splittings. Taking 3 neutrino as an example

$$(m_1^2 - m_2^2) + (m_2^2 - m_3^2) + (m_3^2 - m_1^2) = 0$$

and so one of the mass splittings is defined by the other two.

Taking the LSND result at face value means that there are now *3* independent mass splittings : $\Delta m^2_{12} = 8 \times 10^{-5}\text{eV}^2$, $|\Delta m^2_{23}| = 2.3 \times 10^{-3}\text{eV}^2$ and $|\Delta m^2_{LSND}| = 1.2\text{eV}^2$, implying at least 4 active neutrinos. However the LEP results conclusively showed that there were only 3 neutrino flavours with masses below half the Z^0 boson mass. That means that the other neutrino must be *sterile* i.e. it can't couple to the weak interaction. This new neutrino only couples to gravity, and only appears, fleetingly, during the oscillation process.

9.1.1 Combining with other experiments

The LSND result presents even more difficulties when one tries to combine it with other experiments. A number of different experiments (Bugey, CCFR, CDHS, CHOOZ, KARMEN and NOMAD) have studied oscillations with a $\Delta m^2 \sim 1$ eV^2, albeit mostly looking at ν_μ disappearance rather than $\overline{\nu_e}$ appearance. Under the assumption of CPT invariance and in the two-flavour scheme,

$$P(\nu_\mu \to \nu_\mu) = 1 - P(\nu_\mu \to \nu_e) = 1 - P(\overline{\nu_\mu} \to \overline{\nu_e})$$

So, we should be able to compare previous short-baseline neutrino experiments with the LSND result. This has been done (see Phys.Rev. D70 (2004) 073004) and the results are somewhat discouraging. If one restricts oneself to a single sterile neutrino - the so-called (3+1) scenario - in which the mass patterns look like those in the left pattern of Figure 24 and analyses the world data we find that we can fit the world data into a consistent framework, but the minute we introduce the atmospheric results into the mix we find the results to be highly incompatible. Hence the (3+1) scenario is now disfavoured.

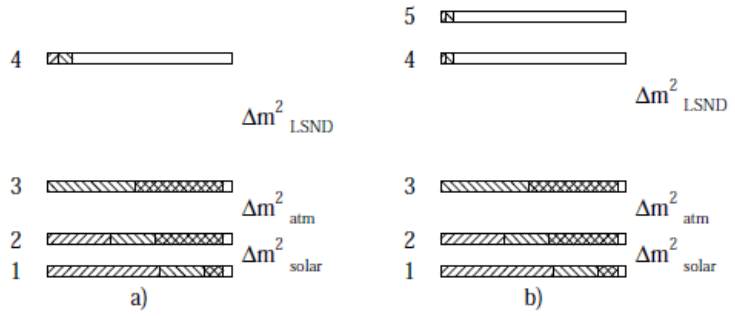

Figure 24: Mass patterns for the (Left) (3+1) scenario and (Right) for (3+2) Scenario. Neutrino masses increase from bottom to top. The ν_e fractions in the mass states are indicated by the right-leaning hatches, the ν_μ content by the left-leaning hatches and the ν_τ content by the crossed hatching. Sterile components are represented by no hatches. Note that the new neutrino states are mostly sterile with a very small mixture of active states.

However, we could just increase the number of sterile states (why not?) and think about a (3+2) scenario (with the mass pattern shown on the right of Figure 24). In this case we find that all our

experiments tend to be more compatible and we can fit the world data into a coherent, if not exactly pretty, picture.

9.1.2 The miniBooNE Experiment

An important part of the scientific method is verification. A controversial result must be able to be verified by an independent experiment. The role of verification of the LSND appearance result fell to the miniBooNE experiment which ran at Fermilab from 2003 to the present. The detector operated in the Fermilab Booster ν_μ beam and looked for ν_e appearance in this beam.

The Booster beam is a standard accelerator-based neutrino beam, generating neutrinos from the decay of pions in flight. It generates ν_μ with energies of approximately 1.0 GeV in a beam which is 99.7% pure. The other 0.3% consists of ν_e which is generated from muon decay in the beam. The miniBooNE detector is a spherical tank containing 800 tons of mineral oil with scintillator doping, just like LSND. The mineral oil is viewed by 1280 photomultiplers. A photograph of part of the inner section of miniBooNE is shown in Figure 25.

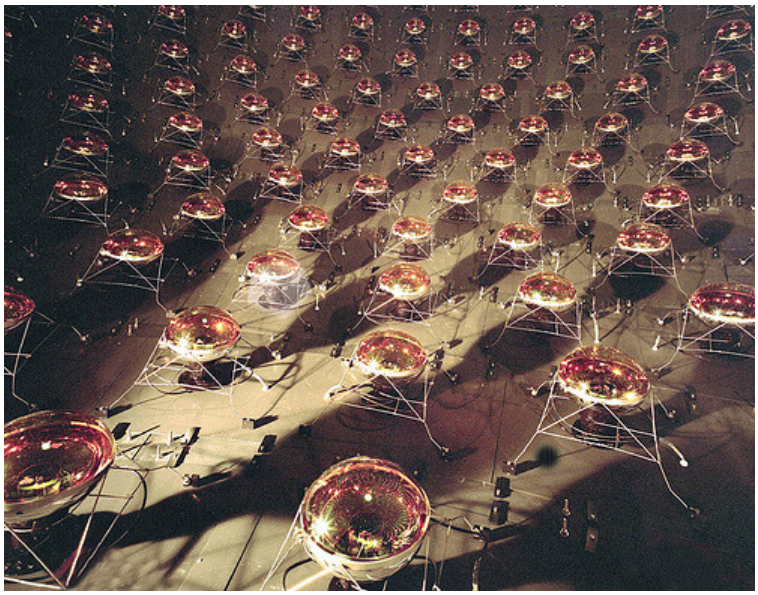

Figure 25: Photograph of an internal section of the miniBooNE tank showing some of the photomultiplers mounted to the walls to view the interactions in the mineral oil.

Positioned 500 m away from the beam, miniBooNE was capable of observing the same mass difference as LSND, but with different systematic effects and in a different, and better understood, neutrino energy regime. The detector looked for ν_e appearance by observing ν_e charged current interactions in the oil.

MiniBooNE released its latest results in 2012. The appearance excess is shown in Figure 26 in neutrino and anti-neutrino running. Although the experiment found no excess of events in the region of the experiment where LSND predicts an excess, it did observe a lower energy excess of events. This new source of excess cannot arise from the LSND parameters - it is too low in energy. Noone is too sure what is causing it at the moment. However, brushing it under the carpet for a moment, if we use the absence of an excess in the LSND region to compute an exclusion region (see Figure 27) we

find that miniBooNE rules out a large fraction of the LSND allowed region, but not, unfortunately, all of it.

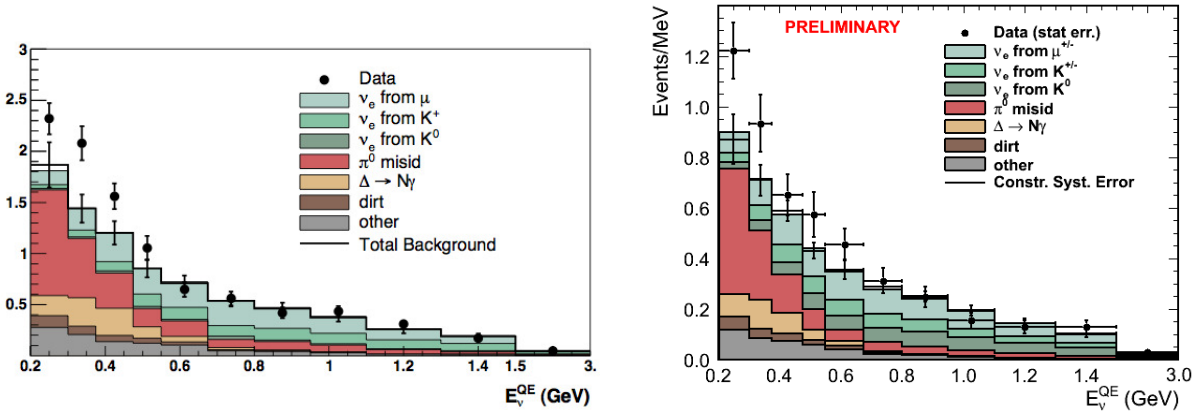

Figure 26: Excess of (left) ν_e and (right) $\overline{\nu_e}$ events observed in the miniBooNE experiment. The dots show the data. The coloured histograms show the expected background from a number of different background sources. Both neutrino and antineutrino data show an excess of events at low energy.

One of the main criticisms of the miniBooNE experiment has always been that it is searching for $\nu_\mu \rightarrow \nu_e$ oscillations whereas LSND was measuring $\overline{\nu_\mu} \rightarrow \overline{\nu_e}$ oscillations. Although CPT symmetries state that the two should have the same probabilities, this sort of loop-hole worries experimentalists. In 2009, the Booster neutrino beam switched to running antineutrinos so that a direct comparison between miniBooNE and LSND could be made. The results are shown in Figure 26. As with the neutrino data, an excess at lower energies is observed (making it more likely to be a result of some unknown background source than oscillations in my humble opinion).

So where are we left with the LSND problem? Unfortunately not much further. We still have an excess in the LSND data, but there is now also a different excess in the miniBoone data. None of this is easy to interpret so the only conclusion we can really make is that we need more data to work out what is going on. The best model that even vaguely fits the data is a (3+2) sterile scenario with large CP violation, but this is all beyond-Standard Model physics.

9.2 The Reactor and Gallium Anomalies

Two other anomalies which may be suggestive of the existance of at least one sterile neutrino have also recently floated into view. The reactor anomaly arose after the introduction of new and very detailed calculations of the $\overline{\nu_e}$ flux from reactors in 2011. Up to that point the prediction of $\overline{\nu_e}$ event rates in reactor experiments very close to the reactor core agreed reasonably well. However, the new flux was approximately 4% larger than earlier calculations. Were this to be correct, it would imply that the reactor data actually displayed a *disappearance* of $\overline{\nu_e}$ by the same 4%. Were this "missing flux" to be attributed to $\overline{\nu_e}$ oscillating to some sterile state, it would have to an oscillation mode with $\Delta m^2 \approx 1$ eV^2. It should be noted that calculating the reactor flux in detail is a very complex problem so it may be that there is still some error in the new calculations. The other anomaly is the so-called *Gallium anomaly*. Here the gallium radiochemical experiments, SAGE and GALLEX, were engaged in some radioactive calibration using a large source of $\overline{\nu_e}$. Again, their observed rates were

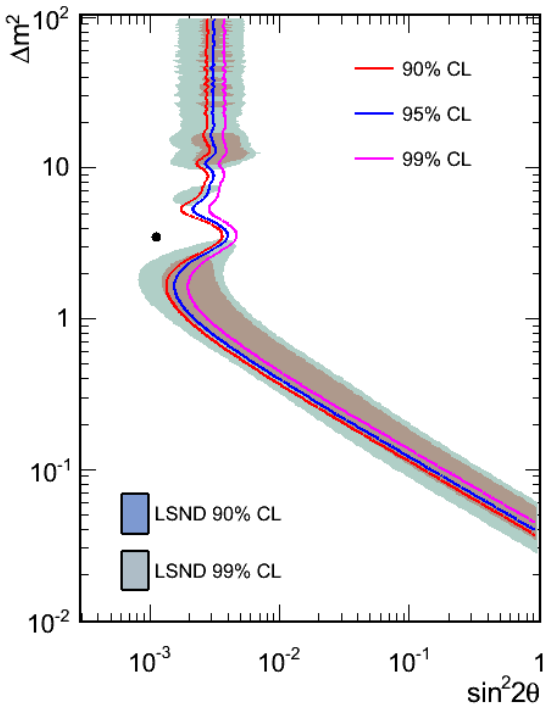

Figure 27: The region of the parameter space excluded by the miniBooNE results. The LSND region is only partially ruled out.

lower than expected given the source activity and, again, this could be interpreted as arising from neutrinos oscillating to some sterile state with $\Delta m^2 \approx 1$ eV^2. Both of these anomalies exist at the 2σ level so it would be wise to view them with some scepticism at the moment. 2-3 σ discrepancies appear, and disappear, with alarming regularity in science.

9.3 What you should know

- What LSND was, what its main result was and what that would imply about neutrinos.
- What the miniBooNE experiment found.
- Brief details of the reactor and Gallium anomalies.

I won't ask for specifics but you should know why these results are controversial.

Now let's brush the whole sterile neutrino issue under a very large carpet and talk about

10 The Future

The measurement of θ_{13} has been a decision point in what neutrino physics does in the future. Since θ_{13} is quite large and accessible, we now want to make precision measurements of the mixing angles. We are left with two parameters to measure : the mass hierarchy and δ_{CP}. We expect the mass hierarchy can be measured in next generation experiments within the next decade or so. The CP violating parameter is a harder measurements and will take a little longer.

10.1 Degeneracies

The main problem we have when attempting to measure the mass hierarchy and δ_{CP} is the fact that the oscillation probabilities are multi-variable functions. That is, the probability for the $\nu_\mu \rightarrow \nu_e$ oscillation mode is, when written generally, a function of all the mixing angles as well as both mass splittings, matter effects, δ_{CP} and the mass hierarchy. A single measurement, however, only give you one number and there are a number of different combinations of these parameters which might return the same number. The problem is afflicted with degeneracies. The effect of these choices can be seen in Figure 28 which shows the neutrino and antineutrino appearance probability for a set of oscillation parameters at a given $L/E = 732/1.5$ km/GeV. Each contour traces out a ellipse in probability space as a function of δ_{CP}. The location of the center of the ellipse on one side of the equal probability line (y=x) is dictated by the mass hierarchy. The distance of the center from the origin is governed by the value of θ_{13}. A single measurement, with errors, of both neutrino and antineutrino probabilities encompasses a set of different possible parameter values.

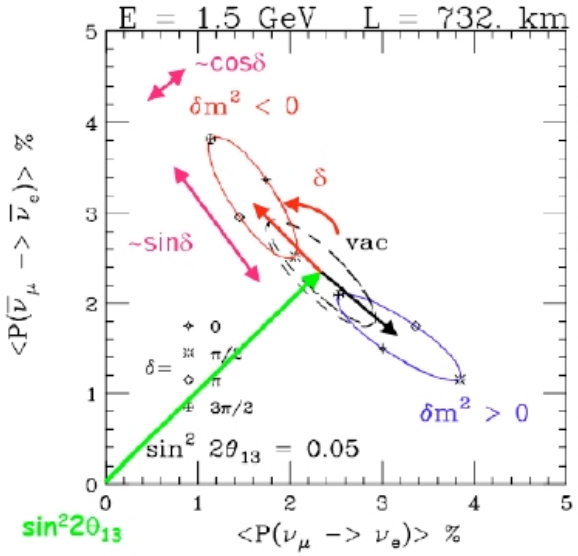

Figure 28: The neutrino and antineutrino appearance probability for a set of oscillation parameters at a given $L/E = 732/1.5$ km/GeV. Each contour traces out a ellipse in probability space as a function of δ_{CP}. The location of the center of the ellipse on one side of the equal probability line (y=x) is dictated by the mass hierarchy. The distance of the center from the origin is goverened by the value of θ_{13}.

In order to unravel these degeneracies one needs more than one experiment at different values of L/E. In addition it helps if those experiments are differently sensitive to mass hierarchy and δ_{CP}.

10.2 Current and future experiments

The two experiments currently operating are T2K in Japan and the NOVA experiment in the USA. T2K, with a baseline of $L/E = 295/0.6$ km/GeV, has only collected about 7% of it's final data set and will therefore be able to do much better at constraining the mixing angles as the size of the data set increases. NOVA uses an upgraded NuMI beam, and directs a ν_μ beam to a detector in Ash River, Northern Minnesota, about 810 km away. It is also an off-axis experiment with an L/E of 810/2.3

km/GeV. Since the far detector is further away than it is in T2K, NOVA is sensitive to effects from the matter in the earth between source and detector, just like the solar experiments. Hence, NOVA can also potentially measure the mass hierarchy in the 23-sector (remember that we know $|\Delta m^2_{23}|$ but not the absolute value). NOVA is starting to produce results now.

The next generation of long baseline experiments are now being designed. The first is Hyper-Kamiokande, a direct upgrade of T2K. Hyper-K still used the water Cerenkov techniques but upgrades the T2K beam to 750 kW and increases the size of the far detector to about half a megaton of water. Hyper-K has the same L/E as T2K. The second experiment is DUNE, which directs an upgraded neutrino beam with an average energy of 3 GeV from Fermilab to a set of large liquid argon TPC detectors 1300 km away in the Homestake mine in South Dakota. For good physics reasons discussed below, DUNE utilises a wide-band, rather than off-axis, beam. The mass of the far detector is only 70 kton (not 500, as in Hyper-K) but this is compensated for by a far more powerful beam (1.2 MW) and more precise detectors. Both experiments are currently in the design and proto-typing phase with the expectation of turning on around 2025 or so.

10.3 Mass hierarchy measurements

The mass hierarchy can be estimate in one of two ways : comparison of the results of two experiments making $\nu_\mu \to \nu_e$ and $\overline{\nu_\mu} \to \overline{\nu_e}$ appearance measurements at different baselines, or by using neutrinoless double beta decay. The current experiments (T2K and NOVA) can do this if they run for about 5 years in neutrino and an equal event rate for antineutrinos. Figure 29 shows that combining T2K and NOVA data we have the potential to determine the mass hierarchy to 2-3 σ over a limited range of δ_{CP}. This can be done in the next 5 years or so.

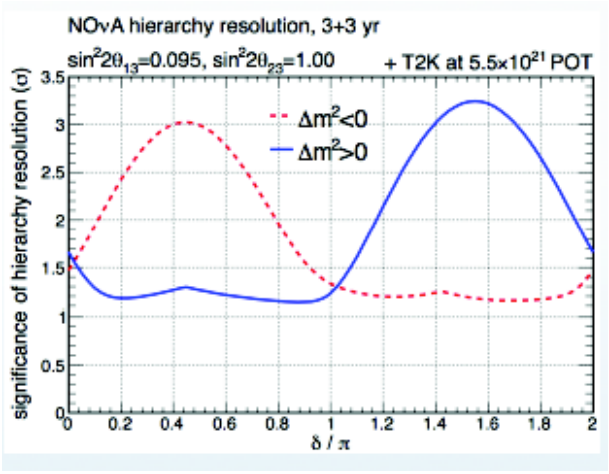

Figure 29: Sensitivity to the mass hierarchy as a function of δ_{CP} if we combine NOVA and T2K data. The plot shows that, with 6 years of NOVA running (3 neutrino and 3 antineutrino) combined with the same for T2K running, we have the potential to determine the mass hierarchy to 2.0 or 3.0 σ over a limited range of δ_{CP}.

If we make the same plot for the next generation of experiments - here we use DUNE - as in Figure 30 we see that the mass hierarchy can be determined to 5 σ over the entire range of δ_{CP} after about 4 years or running. Of course, we need to build DUNE first so this result wouldn't be ready until at least 2025.

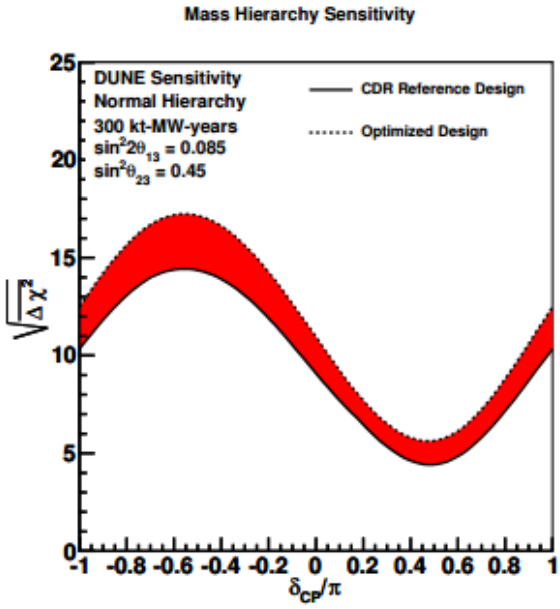

Figure 30: Sensitivity to the mass hierarchy using just the DUNE experiment running for 4 years. The mass hierarchy could be determined to better than 5 σ over the entire range of δ_{CP}.

An alternate way to determine the mass hierarchy is with neutrinoless double beta decay. The interaction rate for this process is proportional to the electron neutrino mass, and hence is proportional to the linear combination of mass states. That is,

$$\Gamma_{0\nu\beta\beta} \propto m_{\nu_e} = \sum_{i=1}^{3} |U_{ei}|^2 m_i = \sum_{i=1}^{3} |U_{ei}|^2 \sqrt{\Delta m^2_{i3} + m^2_3}$$

In the inverted hierarchy, $m_3 \ll m_1 \approx m_2$ and $\Delta m^2_{13} \approx \Delta m^2_{23}$, so we can write

$$m_{\nu_e} = |U_{e1}|^2 \sqrt{\Delta m^2_{23} + m^2_3} + |U_{e2}|^2 \sqrt{\Delta m^2_{23} + m^2_3} + |U_{e3}|^2 m_3$$

Since the lightest mass state, $m_3 > 0$, we have

$$\begin{aligned} m_{\nu_e} &> (|U_{e1}|^2 + |U_{e2}|^2)\sqrt{\Delta m^2_{23}} \\ &= (1 - |U_{e3}|^2)\sqrt{\Delta m^2_{23}} \\ &= cos^2\theta_{13}\sqrt{\Delta m^2_{23}} \end{aligned}$$

where the second last step comes from the fact that the PMNS matrix is unitary. The conclusion is that, if the hierarchy is inverted, the electron neutrino mass m_{ν_e} must have a lower bound. Figure 31 shows the behaviour of the electron neutrino mas, m_{ν_e} as a function of the lightest mass state for the normal and inverted hierarchy. The bands show the spread in m_{ν_e} from different guesses of the Majorana phases in the PMNS matrix (remember the ones we dropped when talking about oscillations?). The behaviour is quite complicated, but the thing to focus on is that, in the case of the inverted hierarchy and at low m_3, $m_{\nu_e} > 0.01$ eV. Hence, if the current or next generation of

neutrinoless double beta decay experiments were able to put a limit on the electron neutrino mass of *less than 0.01 eV* they would be able to rule out the inverted hierarchy. The current experimental limits are an order of magnitude larger so there is work to do - we need larger experiments and longer running time. Of course, this is all predicated on the assumption that the neutrino is a Majorana particle. If it isn't then cannot make this conclusion (we'll never see anything, but that's because there's nothing to see...).

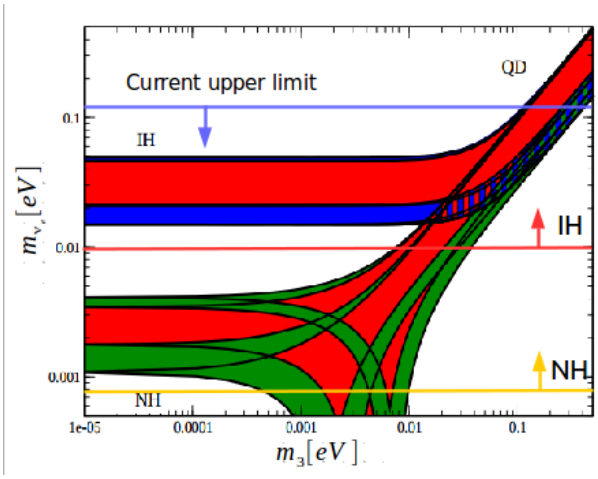

Figure 31: Dependence of the electron neutrino mass, m_{ν_e}, on the lightest mass state for the neutrinoless double beta decay process.

In general we expect that we will know the mass hierarchy by about 2025 or so, with good indications within the next 5 years.

10.4 Measuring δ_{CP}

For reasons we've already discussed (see-saw, leptogenesis, etc) determining if there is CP-violation in the lepton sector is the major goal of the world-wide neutrino programme. Once the mass hierarchy is determined, measurement of δ_{CP} becomes fairly straight forward. Since δ_{CP} only appears as a complex parameter in the PMNS matrix, it can only be accessed by measurements sensitive to the complex nature of the matrix. The flavour change probability is

$$P(\nu_\alpha \to \nu_\beta) = \delta_{\alpha\beta} - 4\sum_{i>j} \Re(U^*_{\alpha i}U_{\beta i}U_{\alpha j}U^*_{\beta i}) sin^2(\Delta m^2_{ij}\frac{L}{4E}) + 2\sum_{i>j} \Im(U^*_{\alpha i}U_{\beta i}U_{\alpha j}U^*_{\beta i}) sin(\Delta m^2_{ij}\frac{L}{4E}) \tag{112}$$

If we are performing a disappearance experiment, then $\alpha = \beta$, and $\Im(U^*_{\alpha i}U_{\beta i}U_{\alpha j}U^*_{\beta i}) = 0$. Hence, any experiment that wants to be sensitive to δ_{CP} has to be an *appearance* experiment.

There are two ways to measure δ_{CP} once the mass hierarchy is known:

1. Measure the flavour change probabilities for $\nu_\mu \to \nu_e$ and $\overline{\nu_\mu} \to \overline{\nu_e}$. As shown in Figure 28, once these probabilities are known sufficiently precisely one can localise δ_{CP} on the ellipse. Hyper-K, which has the use of an off-axis beam, will try to use this method. Figure 32 shows the expected sensitivity of HyperK to δ_{CP} as a function of δ_{CP}. The plot shows that HyperK believes it can state that δ_{CP} is non-zero at $5(3)\sigma$ if $40(20)^\circ < |\delta_{CP}| < 140(160)^\circ$. Doing so, however, requires

us to make precise measurements of the anti-neutrino flavour change probability. In general, with accelerator beams, the flux of antineutrinos tends to be lower than that of neutrinos. Combine this with a cross section for anti-neutrino interacting on a nucleus of only half to a third of neutrino cross section and the observed anti-neutrino event rate can be a factor of 4 or 6 lower than the corresponding neutrino event rate. For the same statistical power, one would have to run in anti-neutrino mode 4 to 6 times longer than the neutrino mode which has cash and scheduling implications (do you have grant for running that long? Will the accelerator complex allow you to do so, etc etc).

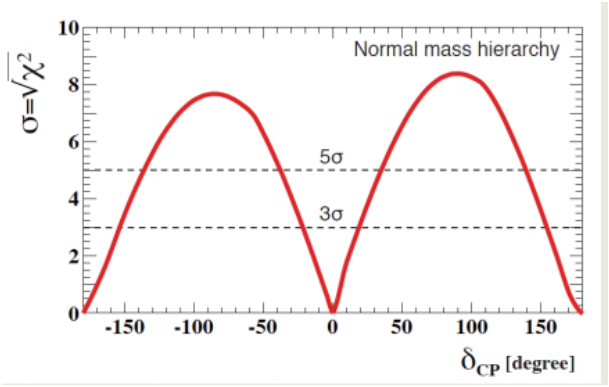

Figure 32: Sensitivity of Hyper-K to non-zero δ_{CP}. The vertical axis measures the zero-δ_{CP} exclusion error.

2. The other method is more subtle but allows you to measure δ_{CP} only using neutrino oscillations, hence speeding up the measurement. The left hand plot in Figure 33 plots the appearance probability, $P(\nu_\mu \to \nu_e)$, as a function of neutrino energy for the DUNE baseline length of 1300 km between source and detector and for different assumed values of δ_{CP}. You can see all the of the θ_{13} oscillation peaks superimposed on top of the solar oscillation line. The important point to note is the difference in size between the first (at a neutrino energy of around 2 GeV) and the second (at around 0.8 GeV) oscillation peaks as a function of δ_{CP}. When δ_{CP} is zero, the two peaks have roughly the sample value. However, if δ_{CP} is $\pm\frac{\pi}{2}$ the first or second peak are larger. Hence, if the experiment is capable of resolving the two peaks one can measure δ_{CP} without requiring antineutrinos. This is what DUNE, which has been designed with a wide-band beam, is designed to do. DUNE's sensitivity to non-zero δ_{CP} can be seen on the right-hand plot of Figure 33. It is quite similar to that from Hyper-K, although may be achieved faster with the wide-band beam.

So, is there any indication of a non-zero δ_{CP}. Actually yes there is. This comes from an analysis by T2K. Figure 34 shows the change in fit χ^2 of a full 3-flavour model with possible non-zero δ_{CP} to a combination of T2K and reactor data. The black and red lines are the normal and inverted mass heirarchies respectively. Ignore the blue lines. What this plot shows is that a better fit is achieved if δ_{CP} is around $-\frac{\pi}{2}$. That is, there are indications that in order to best fit an oscillation model to the T2K and reactor data, δ_{CP} must be non-zero.

This is suggestive, but hardly conclusive. However it does mean that we neutrino experimentalists have something to look forward to as the region of δ_{CP} suggested by T2K and the reactor data is precisely where DUNE and HyperK are most sensitive. We probably will know if δ_{CP} is large by 2025-2030.

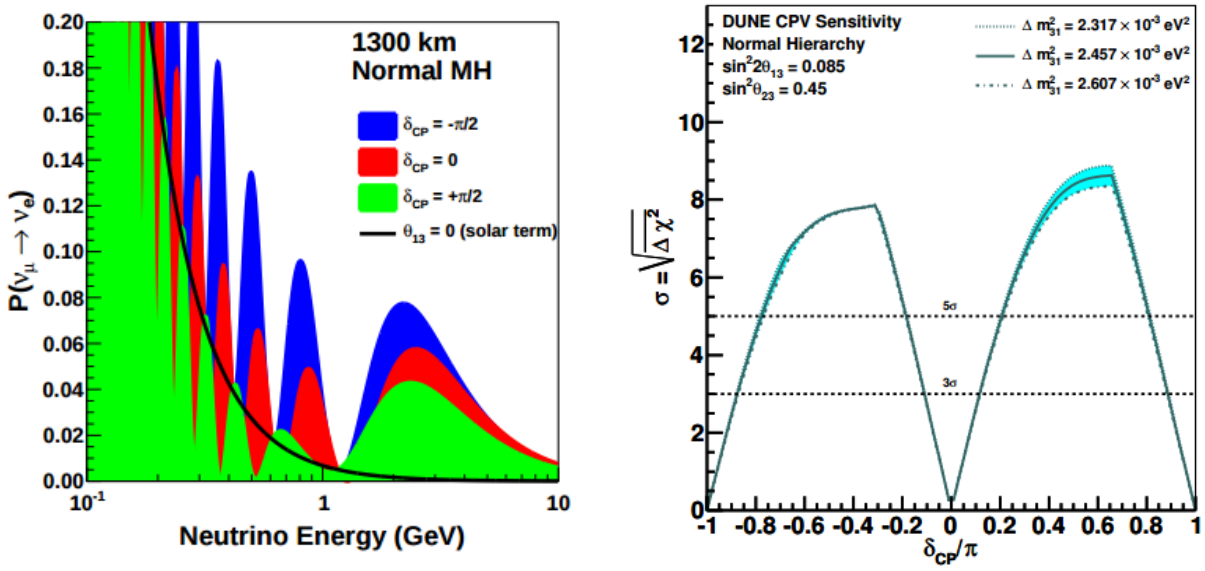

Figure 33: (Left) The appearance probability, $P(\nu_\mu \rightarrow \nu_e)$, as a function of neutrino energy for the DUNE baseline length of 1300 km between source and detector and for different assumed values of δ_{CP} (from DUNE CDR Volume 2). (Right) Sensitivity to non-zero δ_{CP}.

10.5 What you need to know

- Why measuring the mass hierarchy and δ_{CP} is difficult (degeneracies)
- How mass hierarchy and δ_{CP} measurements are done.
- The experiments are planned to measure these. Detailed knowledge of experimental sensitivities is not necessary.

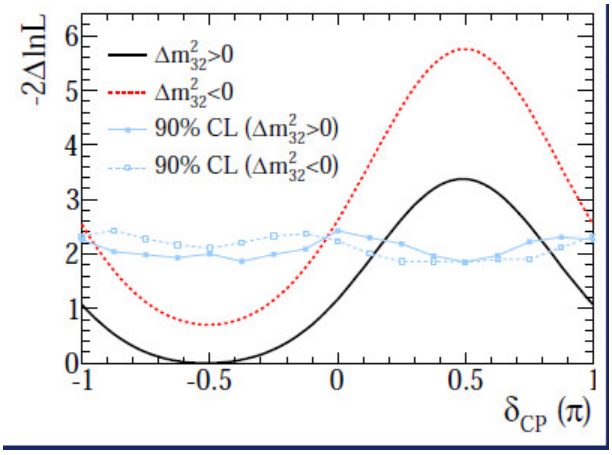

Figure 34: Change in fit χ^2 from minimum χ^2 from a fit of an oscillation model to the T2K and reactor data.